J. Fluid Mech. (1989), *vol.* 208, *pp.* 193–223
Printed in Great Britain

The effect of large-eddy breakup devices on flow noise

By A. P. DOWLING
The University Engineering Department, Trumpington Street, Cambridge CB2 1PZ, UK

(Received 2 August 1988 and in revised form 22 April 1989)

The installation of large-eddy breakup devices (LEBUs) or 'flow manipulators' in a turbulent boundary layer over a rigid plane surface is known to lead to reductions in skin-friction coefficient, turbulence intensity and fluctuating Reynolds stress. We investigate the effect of such devices on the surface pressure spectrum and the far-field sound radiation. A model problem, in which a two-dimensional elliptical vortex is convected past a LEBU, is solved analytically in the low-Mach-number limit. The main noise source mechanisms are identified in this idealized problem and we go on to obtain scaling laws for the sound produced by a turbulent boundary-layer flow over a LEBU. The introduction of a LEBU reduces the strength of the Lighthill quadrupole source terms, but it produces an additional dipole source. However, the pressure fluctuations in this dipole field decay rapidly with distance from a LEBU, and we find that an array of LEBU's could have a beneficial effect on the flow noise for radian frequencies which are large in comparison with $c/30\Delta$, where c is the sound speed and Δ denotes the boundary-layer thickness. At lower frequencies the LEBUs are predicted to increase the flow noise.

1. Introduction

Experiments have shown that large-eddy breakup devices (LEBUs) or 'flow manipulators', consisting of short, thin plates placed in the turbulent boundary layer above an extensive plane wall, can reduce the wall skin-friction coefficient. Since the pioneering work of Hefner, Weinstein & Bushnell (1979) and Corke, Guezennec & Nagib (1979), this reduction in skin friction has been confirmed in many laboratory experiments throughout the world. See Nguyen *et al.* (1984), Bandyopadhyay (1986) or Wilkinson *et al.* (1987) for reviews of this experimental work. Typically a maximum local skin-friction reduction of between 15 and 40% is achieved with some reduction in skin friction persisting over a downstream distance of 100Δ–150Δ, where Δ denotes the boundary-layer thickness. If the wall is long enough in the streamwise direction to exploit this skin-friction reduction and the manipulator is sufficiently thin, the total drag on both the wall and the manipulator may be less than that on the wall without the manipulator. Plesniak & Nagib (1985) undertook a systematic optimization of the manipulator geometry. They found that a tandem arrangement of two plates, one downstream of the other, gave best results when each plate had a length of 1.1Δ and was positioned at a height between 0.4Δ and 0.8Δ above the wall. The performance of the manipulator was relatively insensitive to the streamwise separation between the plates.

There is a great discrepancy between the reported net drag reductions, with reductions varying from as much as 30% (Plesniak & Nagib 1985) to nearly zero (Nguyen, Savill & Westphal 1986). It is clear that the net drag reduction is strongly dependent both on the manipulator geometry and on the characteristics of the

turbulence in the oncoming flow. However, all the experimenters agree that significant local reductions in skin-friction coefficient occur downstream of manipulators. Such a reduction has even been measured on an aircraft in flight (Bertelrud 1986), and a modest drag reduction has been obtained by equipping a flat plate in a towing tank with flow manipulators (Sahlin, Alfredsson & Johansson 1986).

The reduction in skin-friction coefficient downstream of a flow manipulator is accompanied by a corresponding decrease in turbulence intensity, turbulent Reynolds stress and integral lengthscale (Westphal 1986; Bonnet, Delville & Lemay 1987; Coustols, Cousteix & Belanger 1987). The streamwise turbulence intensity and fluctuating Reynolds stress relax back to their unmanipulated values some fifty boundary-layer thicknesses downstream of the LEBU, but the attenuation in the normal component of the turbulence intensity persists for a streamwise length of about 150Δ (Guezennec & Nagib 1985). It is these fluctuating velocities that generate sound in a turbulent boundary layer over a plane wall (Ffowcs Williams 1965) and we might hope that a reduction in turbulence intensity might lead to a corresponding reduction in noise. Such an argument is clearly an over-simplification. Although the introduction of a LEBU might reduce the strength of the quadrupole sources, the LEBU exerts unsteady forces on the fluid and leads to new dipole sources. In general in a low-Mach-number flow the sound field due to dipole sources is stronger than that due to quadrupoles. However, these dipoles produce a centred sound field decaying with distance from the LEBU, while the quadrupole sources are distributed throughout the boundary layer. If the turbulence modification persists over sufficient distances downstream of the LEBU for the additional dipole sound field to have decayed to a negligible level before the turbulence recovers to its unmanipulated form, the introduction of a LEBU could have a beneficial effect on the sound field. Whether a LEBU leads to an increase or a decrease in sound level depends on the relative importance of the additional dipole and the modification to the quadrupole source strength. An encouraging experimental result has been reported by Beeler (1986). He measured the pressure spectrum 70 boundary-layer thicknesses downstream of a LEBU in a turbulent boundary layer and found that the presence of the manipulator reduced the unsteady pressure.

Simple theory can explain the reduction in fluctuating velocities produced by a flow manipulator. Dowling (1985) considered an incident line vortex convected past a LEBU consisting of a single short, flat plate. Vorticity shed from the trailing edge of the manipulator was found to cancel the effect of the incident vortex, leading to a significant reduction in velocity fluctuations near the wall. Atassi & Gebert (1987) went on to consider an incident vorticity wave and an aerofoil-shaped manipulator. Once again shed vorticity reduced velocity fluctuations downstream of the LEBU. Balakumar & Widnall (1986) considered a tandem arrangement of two plates. When the two plates are many chord lengths apart, they produce a reduction that is the square of that for a single plate.

The oncoming flow in these theories satisfies Taylor's hypothesis and so is silent in the absence of a LEBU. The models are therefore too crude to investigate the effect of a turbulence manipulator on flow noise. In this paper we extend the theory of Dowling (1985) by considering a cylindrical vortex of slightly elliptical cross-section convected on a uniform mean flow over an infinite plane wall. Such a vortex rotates under the influence of its own velocity field (Lamb 1932). In a slightly compressible fluid it emits sound and has been used as a basic model of a two-dimensional eddy by Howe (1975). We investigate the way in which the sound field of such an eddy is altered as it is convected past a turbulence manipulator consisting of a single, short, flat plate.

In a low-Mach-number flow, the flow field in the vicinity of a source is essentially incompressible. We solve the inner incompressible problem for the elliptical vortex in §2 and in particular determine the pressure it induces on the plane wall. In the absence of a manipulator the unsteady pressure field is proportional to the square of the vortex strength, Γ, and decays with the inverse-square of distance from the vortex core. When a LEBU is placed at a height h above the plane wall in a flow of mean velocity U_∞, there is an additional term in the pressure perturbation proportional to $\Gamma U_\infty h$ and decaying with the inverse-square of distance from the manipulator. For a vortex representing weak levels of fluctuation, Γ is small in comparison with $U_\infty h$ and the LEBU leads to an enhancement of near-field pressures. The augmented wall pressure is most intense directly underneath the LEBU, the maximum being below the 20% chord point.

Once the incompressible inner field has been determined the theory of vortex sound (Powell 1964; Howe 1975) can be used to determine the distant compressible sound field. This is done in §3. In the absence of the LEBU this pressure perturbation has the form appropriate for a quadrupole source and is proportional to the small eccentricity, ϵ, of the vortex core. All vortical elments satisfying Taylor's hypothesis are silent. When the vortex is convected past a LEBU even the vorticity that convects without change generates sound as it exerts an unsteady force on the LEBU. In free space the unsteady lift on the plate would be an effective dipole (Howe 1976), but for our geometry the equal and opposite image of this dipole in the plane wall completely cancels any surface pressure fluctuations this source might produce. It is apparent from the work of Katzmayer (1922) and Jones (1957) that there is an unsteady suction on the leading edge of the plate proportional to the square of the incident velocity perturbation. We find that this tangential dipole source leads to significant surface pressures. The installation of an LEBU enhances the distant pressure field of the single two-dimensional eddy by a factor $\epsilon^{-1}M^{-1}$, where $M = U_\infty/c$ is the mean flow Mach number. In underwater applications the Mach number is very low (of the order of 0.01) and so this represents a considerable augmentation of the sound field of a single eddy.

This exact problem gives us sufficient physical insight to identify the main sources of sound when a LEBU is placed in a turbulent boundary layer. Now, rather than the single two-dimensional vortex considered in §§ 2 and 3, there are convected three-dimensional eddies distributed throughout the boundary layer. In §4 we obtain scaling laws for the surface pressure spectrum under such a turbulent flow. We find that a LEBU produces an additional centred dipole field, but that at large distances from the LEBU this involves smaller pressure fluctuations than those due to the extensive quadrupole sources distributed throughout the boundary layer.

A LEBU reduces the fluctuating velocity over a downstream extent of some 150Δ, and a global reduction in quadrupole source strength could be obtained by an array of LEBUs with a streamwise separation of about 150Δ. We predict that such an array could only lead to local reductions in the surface pressure spectrum for radian frequencies much greater than $c/30\Delta$.

2. The inner incompressible flow field

2.1. *In the absence of a LEBU*

Consider the model of a turbulent eddy in a boundary layer illustrated in figure 1. A two-dimensional vortex with a slightly elliptical core is convected parallel to a rigid plane wall $y_2 = 0$ in a uniform mean flow $(U_\infty, 0, 0)$. At time $t = 0$, the centre of the vortex is at a height d above the wall and we shall denote its streamwise position

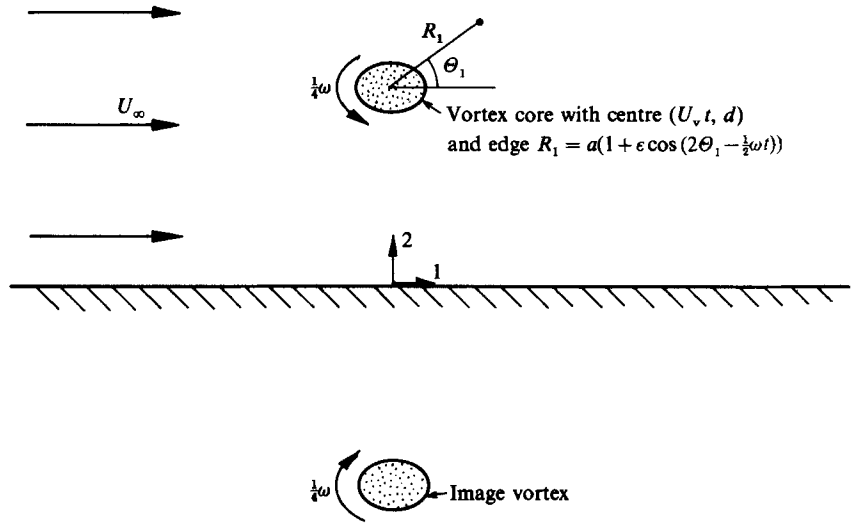

FIGURE 1. An elliptical vortex convected parallel to the rigid wall $y_2 = 0$.

by $y_1 = 0$. Let us suppose that, at this time, the vorticity has a uniform value $(0, 0, \omega)$ within the vortex core and that the outer edge of the core is described by $R_1 = a(1+\epsilon\cos 2\Theta_1)$, where R_1 and Θ_1 are polar coordinates measured from the vortex centreline. In a boundary-layer flow ω would in general be negative. ϵ is a small parameter describing the eccentricity of the ellipse.

In unbounded space in an otherwise quiescent fluid, Lamb (1932) has shown that, to first order in ϵ, such a vortex rotates about its axis with angular velocity $\frac{1}{4}\omega$. The vorticity distribution at a general time t is therefore given by

$$\boldsymbol{\omega} = \omega \boldsymbol{k} H[a + \epsilon a \cos(2\Theta_1 - \tfrac{1}{2}\omega t) - R_1], \tag{2.1}$$

where $\boldsymbol{k}$ is a unit vector in the 3-direction and $H(x)$ is the Heaviside function. The associated velocity field, in polar coordinates based on the vortex axis, is

$$v_R = -\tfrac{1}{2}\epsilon\omega R_1 \sin(2\Theta_1 - \tfrac{1}{2}\omega t), \quad v_\Theta = \tfrac{1}{2}\omega R_1 - \tfrac{1}{2}\epsilon\omega R_1 \cos(2\Theta_1 - \tfrac{1}{2}\omega t) \tag{2.2}$$

inside the vortex core,

$$v_R = -\frac{\epsilon\Gamma a^2}{2\pi R_1^3}\sin(2\Theta_1 - \tfrac{1}{2}\omega t), \quad v_\Theta = \frac{\Gamma}{2\pi R_1} + \frac{\epsilon\Gamma a^2}{2\pi R_1^3}\cos(2\Theta_1 - \tfrac{1}{2}\omega t) \tag{2.3}$$

outside the vortex core, where $\Gamma = \pi a^2\omega$ is the total vortex strength and terms of order ϵ^2 have been neglected.

In our problem there are additional terms in the velocity field due to the mean flow and the image of the vortex in the hard surface. These cause the vortex axis to move with a velocity $(U_v, 0, 0)$, where $U_v = U_\infty + \Gamma/4\pi d$. If a/d is small, this velocity is uniform over the vortex core and the vortex convects without dispersion. The vorticity distribution therefore continues to have the same form as in (2.1), provided R_1 and Θ_1 are measured from the instantaneous position of the vortex axis and we can use Lamb's result to write the velocity field in $y_2 \geqslant 0$:

$$\boldsymbol{v} = \left(U_\infty + \frac{\Gamma}{4\pi d}, 0, 0\right) + \tfrac{1}{2}\omega R_1(-\sin\Theta_1, \cos\Theta_1, 0) - \tfrac{1}{2}\epsilon\omega R_1(\sin(\Theta_1 - \tfrac{1}{2}\omega t), \cos(\Theta_1 - \tfrac{1}{2}\omega t), 0) \tag{2.4}$$

inside the vortex core,

$$\begin{aligned} \boldsymbol{v} = {} & (U_\infty, 0, 0) \\ & + \frac{\Gamma}{2\pi R_1}(-\sin\Theta_1, \cos\Theta_1, 0) + \frac{\epsilon\Gamma a^2}{2\pi R_1^3}(-\sin(3\Theta_1 - \tfrac{1}{2}\omega t), \cos(3\Theta_1 - \tfrac{1}{2}\omega t), 0) \\ & - \frac{\Gamma}{2\pi R_2}(-\sin\Theta_2, \cos\Theta_2, 0) - \frac{\epsilon\Gamma a^2}{2\pi R_2^3}(-\sin(3\Theta_2 + \tfrac{1}{2}\omega t), \cos(3\Theta_2 + \tfrac{1}{2}\omega t), 0) \end{aligned} \quad (2.5)$$

outside the vortex core, where R_2 and Θ_2 are polar coordinates measured from the instantaneous position of the axis of the image vortex. This velocity distribution will be used in §3 to evaluate the sound source terms, but for now we shall go on to determine the inner incompressible pressure fluctuations.

The near-field pressure perturbations can be calculated from the unsteady form of Bernoulli's equation:

$$p' = -\rho_0 \dot{\phi} + \tfrac{1}{2}\rho_0(U_\infty^2 - v^2). \quad (2.6)$$

The dot denotes a time derivative, v is the magnitude of $\boldsymbol{v}$, and ρ_0 is the fluid density. It is apparent from (2.5) that outside the vortex core the velocity potential ϕ is given by

$$\phi = U_\infty y_1 + \frac{\Gamma}{2\pi}(\Theta_1 - \Theta_2) + \frac{\epsilon\Gamma a^2}{4\pi}\left[\frac{1}{R_1^2}\sin(2\Theta_1 - \tfrac{1}{2}\omega t) - \frac{1}{R_2^2}\sin(2\Theta_2 + \tfrac{1}{2}\omega t)\right]. \quad (2.7)$$

The pressure fluctuations on the plane surface $y_2 = 0$ are of particular relevance since they would be detected by a wall-mounted sonar array. There,

$$R_1 = R_2 = [(y_1 - U_v t)^2 + d^2]^{\frac{1}{2}}, \quad \Theta_1 = -\Theta_2 \quad \text{with} \quad \tan\Theta_1 = -d/(y_1 - U_v t),$$

the velocity potential simplifies, and differentiation with respect to time shows that

$$\dot{\phi}(y_1, 0, y_3, t) = -\frac{\Gamma U_v}{\pi}\frac{d}{(y_1 - U_v t)^2 + d^2} - \frac{\epsilon\Gamma^2}{4\pi^2}\frac{\cos(2\Theta_1 - \tfrac{1}{2}\omega t)}{(y_1 - U_v t)^2 + d^2} + O\left(\frac{\epsilon\Gamma U_v a^2}{d^3}\right). \quad (2.8)$$

The normal velocity v_2 of course vanishes on $y_2 = 0$, while the streamwise velocity reduces to

$$v_1 = U_\infty + \frac{\Gamma}{\pi}\frac{d}{(y_1 - U_v t)^2 + d^2} + O\left(\frac{\epsilon\Gamma a^2}{d^3}\right). \quad (2.9)$$

Substitution for $\boldsymbol{v}$ and $\dot{\phi}$ in (2.6) shows that the pressure perturbation on the wall is

$$p'(y_1, 0, y_3, t) = \frac{\rho_0\Gamma^2}{4\pi^2}\frac{\cos 2\Theta_1 + \epsilon\cos(2\Theta_1 - \tfrac{1}{2}\omega t)}{(y_1 - U_v t)^2 + d^2}, \quad (2.10)$$

where

$$\cos 2\Theta_1 = \frac{(y_1 - U_v t)^2 - d^2}{(y_1 - U_v t)^2 + d^2}.$$

The unsteady pressure is evidently proportional to the square of the vortex strength and decays with the inverse-square of distance from the axis of the vortex.

2.2. *With a LEBU*

The way in which the insertion of a flow manipulator or LEBU modifies this flow field will now be investigated. The geometry is illustrated in figure 2. A flat plate LEBU of chord $2l$ and with infinite span is placed at a height h above the plane wall in the two-dimensional flow. Let us denote the position of the vortex centreline at time t by

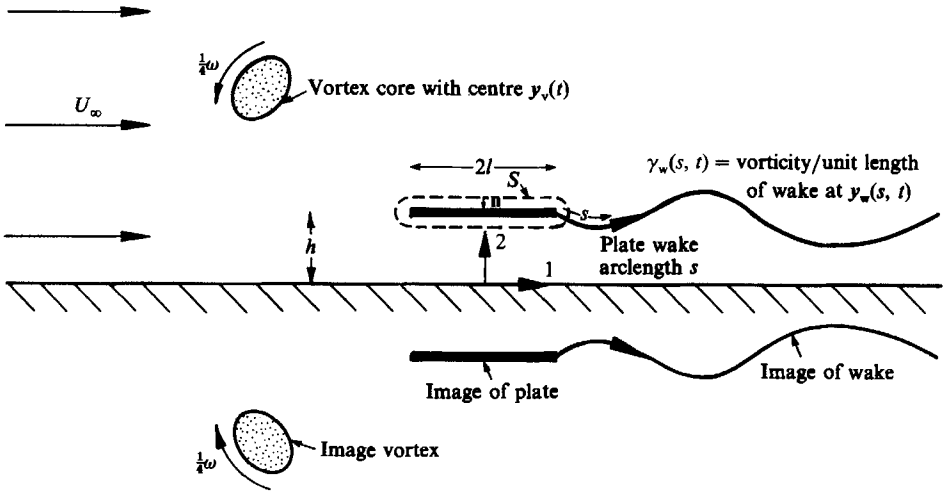

FIGURE 2. An elliptical vortex convected past a LEBU.

$y_v(t)$. At $t = 0$, $y_v = (0, d)$, that is the vortex axis is at a height d above the wall, or equivalently at a distance $b = d - h$ above the LEBU. At this time the outer edge of the vortex core is again described by $R_1 = a + \epsilon a \cos 2\Theta_1$, where R_1 and Θ_1 are polar coordinates based on the vortex axis.

We shall assume that the Reynolds number is sufficiently high for the effects of the fluid's viscosity to be ignored explicitly in the analysis. The dominant influence of viscosity will, however, be implicitly included through the application of the Kutta condition at the trailing edge of the LEBU. The effect of the LEBU can then be represented by a vorticity distribution along the plate; $f(y_1, t)$, $-l \leqslant y_1 \leqslant l$. The function $f(y_1, t)$ is equal to the jump in v_1 across the plate and is to be determined from a condition of no normal velocity on the plate and the Kutta condition. As in Dowling (1985) it is convenient to expand $f(y_1, t)$ as a Glauert series and we write

$$f(y_1, t) = \frac{(l+y_1)}{2l} f(l, t) - \frac{\Gamma}{2l} A_0(t) \cot \tfrac{1}{2}\theta + \frac{\Gamma}{l} \sum_{m=1}^{\infty} A_m \sin m\theta, \tag{2.11}$$

where $\cos\theta = -y_1/l$. The A_0 term has the required form for the singularity at the leading edge of the plate.

As the circulation around the plate changes as a function of time, vorticity is shed unsteadily into the wake, where it convects with the flow. We measure arclength along the wake by s and denote the vorticity per unit length of wake by $\gamma_w(s, t)$ and its position by $y_w(s, t)$. Kelvin's circulation theorem requires that the total circulation around the plate and wake should vanish:

$$\int_0^\infty \gamma_w(s, t)\, \mathrm{d}s = -\int_{-l}^{l} f(y_1, t)\, \mathrm{d}y_1. \tag{2.12}$$

Provided that the size of the vortex core a is small in comparison with the distances d and b, the vortex continues to rotate with angular velocity $\frac{1}{4}\omega$ as it convects without dispersion. The vorticity in the oncoming vortex therefore has the form shown in (2.1), while there is additional vorticity in the wake of the plate. Hence

$$\omega = \omega \boldsymbol{k} H[a + \epsilon a \cos(2\Theta_1 - \tfrac{1}{2}\omega t) - R_1] + \boldsymbol{k} \int_{s=0}^{\infty} \gamma_w(s, t)\, \delta[\boldsymbol{y} - \boldsymbol{y}_w(s, t)]\, \mathrm{d}s \tag{2.13}$$

for $y_2 \geqslant 0$. Inclusion of the effects of the LEBU and its wake into (2.4) shows that within the vortex core the velocity field is given by

$$\begin{aligned} \boldsymbol{v}(\boldsymbol{y},t) = &\left(U_\infty + \frac{\Gamma}{4\pi y_{v2}}, 0, 0\right) + \tfrac{1}{2}\omega R_1(-\sin\Theta_1, \cos\Theta_1, 0) \\ &- \tfrac{1}{2}\epsilon\omega R_1(\sin(\Theta_1 - \tfrac{1}{2}\omega t), \cos(\Theta_1 - \tfrac{1}{2}\omega t), 0) \\ &+ \frac{1}{2\pi}\int_{-l}^{l} f(y_1', t)\{\boldsymbol{E}(\boldsymbol{y}_v \mid y_1', h) - \boldsymbol{E}(\boldsymbol{y}_v \mid y_1', -h)\}\,\mathrm{d}y_1' \\ &+ \frac{1}{2\pi}\int_0^\infty \gamma_w(s,t)\{\boldsymbol{E}(\boldsymbol{y}_v \mid \boldsymbol{y}_w) - \boldsymbol{E}(\boldsymbol{y}_v \mid y_{w1}, -y_{w2})\}\,\mathrm{d}s. \end{aligned} \tag{2.14}$$

Outside the vortex core an extension of (2.5) shows that the corresponding velocities are

$$\begin{aligned} \boldsymbol{v}(\boldsymbol{y},t) = &(U_\infty, 0, 0) \\ &+ \frac{\Gamma}{2\pi R_1}(-\sin\Theta_1, \cos\Theta_1, 0) + \frac{\epsilon\Gamma a^2}{2\pi R_1^3}(-\sin(3\Theta_1 - \tfrac{1}{2}\omega t), \cos(3\Theta_1 - \tfrac{1}{2}\omega t), 0) \\ &- \frac{\Gamma}{2\pi R_1}(-\sin\Theta_2, \cos\Theta_2, 0) - \frac{\epsilon\Gamma a^2}{2\pi R_2^3}(-\sin(3\Theta_2 + \tfrac{1}{2}\omega t), \cos(3\Theta_2 + \tfrac{1}{2}\omega t), 0) \\ &+ \frac{1}{2\pi}\int_{-l}^{l} f(y_1', t)\{\boldsymbol{E}(\boldsymbol{y} \mid y_1', h) - \boldsymbol{E}(\boldsymbol{y} \mid y_1', -h)\}\,\mathrm{d}y_1' \\ &+ \frac{1}{2\pi}\int_0^\infty \gamma_w(s,t)\{\boldsymbol{E}(\boldsymbol{y} \mid \boldsymbol{y}_w) - \boldsymbol{E}(\boldsymbol{y} \mid y_{w1}, -y_{w2})\}\,\mathrm{d}s, \end{aligned} \tag{2.15}$$

where the vector $\boldsymbol{E}(\boldsymbol{y} \mid \boldsymbol{y}')$ is defined by

$$\boldsymbol{E}(\boldsymbol{y} \mid \boldsymbol{y}') = (-(y_2 - y_2'), y_1 - y_1', 0)/((y_1 - y_1')^2 + (y_2 - y_2')^2).$$

The vorticity distribution described in (2.13) and the velocity field in (2.14) and (2.15) will be used in §3 to calculate the pressure fluctuations in the distant sound field. But first we determine the local pressure perturbations on the plane wall near the manipulator, where the flow is essentially incompressible. These near-field pressures can be calculated from Bernoulli's equation:

$$p' = -\rho_0\dot{\phi} + \tfrac{1}{2}\rho_0(U_\infty^2 - v^2)$$

as given in (2.6).

It is apparent from (2.15) that well outside the vortex core the velocity potential has the form

$$\begin{aligned} \phi(\boldsymbol{y},t) = U_\infty y_1 + \frac{\Gamma}{2\pi}(\Theta_1 - \Theta_2) + \frac{1}{2\pi}\int_{-l}^{l} f(y_1', t)\,(\Theta(\boldsymbol{y} \mid y_1', h) - \Theta(\boldsymbol{y} \mid y_1', -h))\,\mathrm{d}y_1' \\ + \frac{1}{2\pi}\int_0^\infty \gamma_w(s,t)\,(\Theta(\boldsymbol{y} \mid \boldsymbol{y}_w(s,t)) - \Theta(\boldsymbol{y} \mid y_{w1}, -y_{w2}))\,\mathrm{d}s, \end{aligned} \tag{2.16}$$

where $\Theta(\boldsymbol{y} \mid \boldsymbol{y}')$ is defined by

$$\tan\Theta = (y_2 - y_2')/(y_1 - y_1') \quad \text{with} \quad \cos\Theta = (y_1 - y_1')/((y_1 - y_1')^2 + (y_2 - y_2')^2)^{\frac{1}{2}}.$$

We now linearize in the strength of the oncoming vortex. Then Γ, f and γ_w are all small and any terms multiplying them need only be evaluated to lowest order in Γ. Explicitly we assume that $1 \gg \Gamma/U_\infty d \gg a/b \gg \epsilon$. Then the incident vortex and

the vorticity in the wake convect with the mean velocity. Hence $\boldsymbol{y}_v = (U_\infty t, d)$, $\boldsymbol{y}_w(s,t) = (s+l, h)$ and

$$\dot{\gamma}_w = -U_\infty \frac{\partial \gamma_w}{\partial s}. \tag{2.17}$$

The velocity field and the velocity potential simplify for this vortex of linear strength. The details are given in Appendix A, where it is shown that substitution for $\boldsymbol{v}$ and ϕ, from (2.15) and (2.16) respectively, into the unsteady Bernoulli equation (2.6) leads to

$$p'(y_1, 0, y_3, t) = -\frac{\rho_0 h}{\pi} \int_{-l}^{l} \frac{g(y_1', t) + U_\infty f(y_1', t)}{(y_1 - y_1')^2 + h^2} \mathrm{d}y_1', \tag{2.18}$$

after linearization in Γ. A new function $g(y_1, t)$ has been introduced in this expression. It is defined by

$$g(y_1, t) = \int_{-l}^{y_1} \dot{f}(y_1', t)\, \mathrm{d}y_1'. \tag{2.19}$$

The surface pressure evidently depends on the functions f and g and decays with the inverse square of distance from the plate. For a complete description it only remains to calculate f and g.

In (2.11) f was expanded as a Glauert series. The function g can be expressed in terms of the same coefficients. After substitution for f in terms of its series and evaluation of the integrals, (2.19) leads to

$$g(y_1, t) = \frac{1}{4l}(y_1 + l)^2 \dot{f}(l, t) - \tfrac{1}{2}\Gamma \dot{A}_0(\theta + \sin\theta) + \tfrac{1}{2}\Gamma \dot{A}_1(\theta - \tfrac{1}{2}\sin 2\theta) + \sum_{n=2}^{\infty} \tfrac{1}{2}\Gamma \dot{A}_n \left(\frac{\sin(n-1)\theta}{n-1} - \frac{\sin(n+1)\theta}{n+1} \right), \tag{2.20}$$

where $\cos\theta = -y_1/l$.

The functions $A_n(t)$ are to be determined from the condition of zero normal velocity on the plate, which after linearization of (2.15) leads to the following integral equation for f:

$$\oint_{-l}^{l} f(y', t) \left\{ \frac{1}{y_1 - y_1'} - \frac{y_1 - y_1'}{(y_1 - y_1')^2 + 4h^2} \right\} \mathrm{d}y_1' = -\Gamma \frac{y_1 - U_\infty t}{(y_1 - U_\infty t)^2 + b^2} + \Gamma \frac{y_1 - U_\infty t}{(y_1 - U_\infty t)^2 + (b+2h)^2} - \int_0^\infty \gamma_w(s, t) \left\{ \frac{1}{y_1 - s - l} - \frac{y_1 - s - l}{(y_1 - s - l)^2 + 4h^2} \right\} \mathrm{d}s, \tag{2.21}$$

where $\oint$ denotes a principal value, and $b = d - h$ is the perpendicular distance between the LEBU and the axis of the vortex at time $t = 0$. Terms of order $\epsilon \Gamma a^2/b^3$ have been neglected. This is precisely the equation solved in Dowling (1985) and we need only quote the results derived there. It was found to be convenient to take Fourier transforms with respect to a non-dimensional time, $U_\infty t/l$. With $\hat{A}_n(\Omega)$ defined by

$$\hat{A}_n(\Omega) = \frac{U_\infty}{l} \int_{-\infty}^{\infty} A_n(t)\, \mathrm{e}^{\mathrm{i}\Omega U_\infty t/l}\, \mathrm{d}t, \tag{2.22}$$

Dowling showed that the integral equation (2.21) leads to an infinite set of linear coupled equations for the Glauert coefficients $\hat{A}_n$ (see Dowling 1985, equation (3.9)),

$$\hat{A}_n - \hat{A}_0(C_{0,n} + C_{1,n}) + \sum_{m=1}^{\infty} \hat{A}_m (C_{m-1,n} - C_{m+1,n}) + (\hat{A}_0 - \hat{A}_1) S_n = -2\mathrm{i}^{-n+1} J_n(\Omega) [\mathrm{e}^{-\Omega|b|/l} - \mathrm{e}^{-\Omega(b+2h)/l}], \tag{2.23}$$

for $n \geqslant 0$ and positive Ω. In this expression

$$C_{m,n} = \frac{1}{\pi}\int_0^{\pi} \cos n\theta\, E_m(-\cos\theta)\,\mathrm{d}\theta,$$

$$S_n = \frac{\mathrm{i}\Omega}{1-\mathrm{i}\Omega}\left[s_n + \frac{1}{2}\int_{-1}^{1}(1+x)\,E_n(x)\,\mathrm{d}x + \mathrm{e}^{-1\Omega}\int_1^{\infty}\mathrm{e}^{\mathrm{i}\Omega x}\left\{E_n(x) - \frac{[(x^2-1)^{\frac{1}{2}}-x]^n}{(x^2-1)^{\frac{1}{2}}}\right\}\mathrm{d}x\right],$$

with

$$E_n(x) = \frac{1}{\pi}\int_0^{\pi}\frac{\cos m\theta'(x+\cos\theta')}{(x+\cos\theta')^2+4h^2/l^2}\,\mathrm{d}\theta'$$

and $s_0 = 0$, $s_1 = -1$, $s_n = [(-1)^n(2n^2-1)+1]/2n(n^2-1)$ for $n \geqslant 2$. The $\hat{A}_n$ decay rapidly as n becomes large, and Dowling determined these coefficients approximately by truncating the series after N terms. Then the first N equations in (2.23) could be solved numerically to give the N unknowns $\hat{A}_0, \hat{A}_1, \ldots, \hat{A}_{N-1}$. In addition Dowling showed that the Kutta condition implied that

$$\hat{f}(l,\Omega) = \frac{\mathrm{i}\pi\Gamma\Omega}{2l(1-\mathrm{i}\Omega)}(\hat{A}_1(\Omega) - \hat{A}_0(\Omega)), \tag{2.24}$$

so that knowledge of the $\hat{A}_n$ completely specifies the functions f and g via equations (2.11) and (2.20) respectively.

When h is sufficiently large and b is positive, the plate is far enough from the wall for images in the plane wall to have negligible effect on the circulation around the plate. The plate then responds to the passage of the vortex as if it were in unbounded space, and the coefficients $\hat{A}_n$ can be calculated analytically. If $h \gg \frac{1}{2}l$ the coupling coefficients $C_{m,n}$ are small, and the equations for $\hat{A}_n$ in (2.23) decouple to give, in particular,

$$\hat{A}_1 - \hat{A}_0 = \frac{4\mathrm{i}(1-\mathrm{i}\Omega)}{\pi\Omega}\frac{J_0(\Omega)+\mathrm{i}J_1(\Omega)}{H_0^{(1)}(\Omega)+\mathrm{i}H_1^{(1)}(\Omega)}\mathrm{e}^{\mathrm{i}\Omega-\Omega|b|/l}, \tag{2.25}$$

$$\hat{A}_0 = -\frac{4\mathrm{i}}{\pi\Omega}\frac{\mathrm{e}^{-\Omega|b|/l}}{H_0^{(1)}(\Omega)+\mathrm{i}H_1^{(1)}(\Omega)} \tag{2.26}$$

and

$$\hat{A}_2 = -\frac{4\mathrm{i}(\Omega-2\mathrm{i})}{\pi\Omega^2}\frac{\mathrm{e}^{-\Omega|b|/l}}{H_0^{(1)}(\Omega)+\mathrm{i}H_1^{(1)}(\Omega)} + \frac{8(1-\mathrm{i}\Omega-\frac{1}{3}\Omega^2)}{\pi\Omega^2}\frac{J_0(\Omega)+\mathrm{i}J_1(\Omega)}{H_0^{(1)}(\Omega)+\mathrm{i}H_1^{(1)}(\Omega)}\mathrm{e}^{\mathrm{i}\Omega-\Omega|b|/l} \tag{2.27}$$

for $\Omega > 0$.

We now return to the evaluation of the surface pressure fluctuations. Taking Fourier transforms of (2.18) we find that

$$\hat{p}(y_1,0,y_3,\Omega) = -\frac{\rho_0 h}{\pi}\int_{-l}^{l}\frac{\hat{g}(y_1',\Omega)+U_\infty\hat{f}(y_1',\Omega)}{(y_1-y_1')^2+h^2}\,\mathrm{d}y_1'. \tag{2.28}$$

This integral only involves known functions, since f and g have been expressed in terms of the Glauert coefficients A_n via (2.11), (2.20) and (2.24), while the A_n are determined by a numerical solution of (2.23). It is possible to evaluate the integrals involved in (2.28) analytically but the expressions are so cumbersome that a numerical integration is preferable. Figure 3 shows the variation of $\hat{p}(y,\Omega)$ with

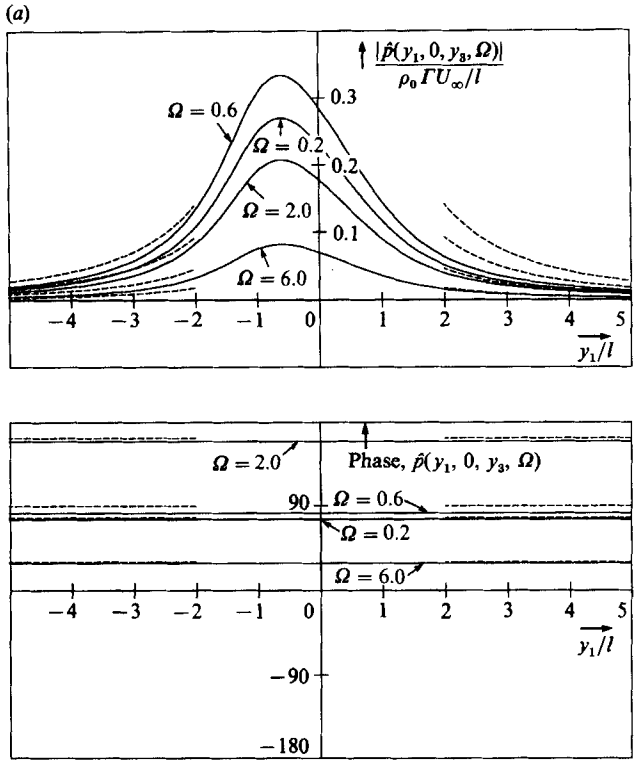

FIGURE 3(*a*). For caption see facing page.

position along the wall for various values of Ω and two values of h/l. At each frequency the pressure perturbation is in phase all along the wall, as is appropriate for an incompressible flow where information travels instantaneously. The maximum pressure perturbation occurs at the same streamwise location for all frequencies. For $h = l$ this is at $y_1 = -0.6l$, i.e. directly below the 20% chord point. For $h = \frac{1}{2}l$, the maximum pressure occurs slightly further upstream at $y_1 = -0.7l$. The figure shows that, as the frequency increases, the amplitude of the pressure oscillations first increases and then decreases. For the values of h in the figure, the largest pressure response occurs for non-dimensional frequencies Ω in the range $0.6 < \Omega < 2.0$. (Frequencies have been non-dimensionalized with respect to U_∞/l.)

The expression for the surface pressure simplifies at many chord lengths from the plate. When $|y_1|$ is large in comparison with $2l$, (2.28) becomes

$$\hat{p}(y_1, 0, y_3, \Omega) = -\frac{\rho_0}{\pi} \frac{h}{y_1^2 + h^2} \int_{-l}^{l} [\hat{g}(y_1', \Omega) + U_\infty \hat{f}(y_1', \Omega)] \, \mathrm{d}y_1' \left(1 + O\left(\frac{2l}{|y_1|}\right)\right). \quad (2.29)$$

When $\hat{f}$ and $\hat{g}$ are replaced by their series expansions (given in (2.11) and (2.20)) the integrals can be evaluated to show

$$\hat{p}(y_1, 0, y_3, \Omega) = -\frac{\rho_0 U_\infty}{\pi} \frac{h}{y_1^2 + h^2} [l\hat{f}(l, \Omega)\,(1 - \tfrac{2}{3}\mathrm{i}\Omega) + \tfrac{1}{2}\pi\Gamma(\hat{A}_1 - \hat{A}_0)\,(1 - \mathrm{i}\Omega) + \tfrac{1}{4}\pi\Gamma\mathrm{i}\Omega(\hat{A}_0 - \hat{A}_2)]. \quad (2.30)$$

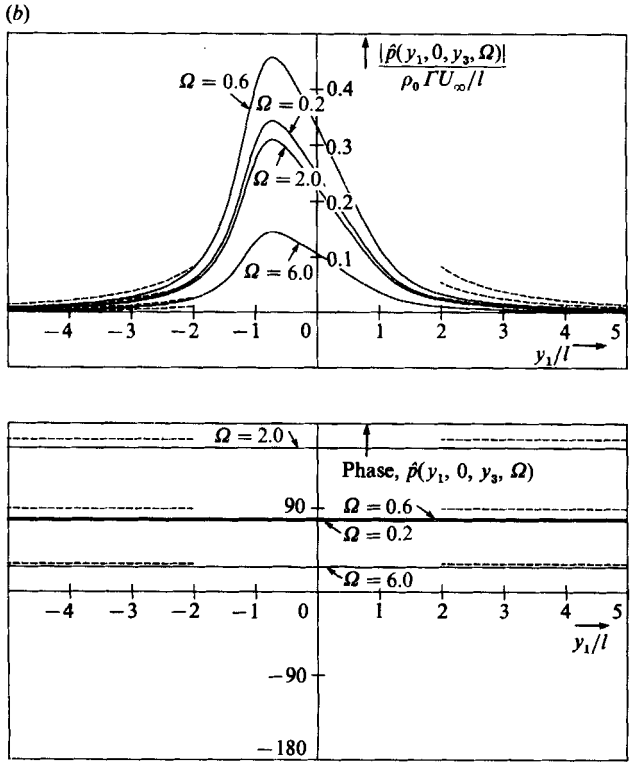

FIGURE 3. The variation of the Fourier transform of the pressure perturbation with position along the wall for various non-dimensional frequencies, $b = 0.1l$ and (*a*) $h = l$, (*b*) $h = 0.5l$: ——, calculated from (2.28); --------, calculated from the approximate form for moderate or large h/l in (2.32).

After substitution for $\hat{f}(l, \Omega)$ from (2.24) this becomes

$$\hat{p}(y_1, 0, y_3, \Omega) = -\tfrac{1}{2}\rho_0 \Gamma U_\infty \frac{h}{y_1^2 + h^2}\left[\frac{\hat{A}_1 - \hat{A}_0}{1 - \mathrm{i}\Omega}(1 - \mathrm{i}\Omega - \tfrac{1}{3}\Omega^2) + \tfrac{1}{2}\mathrm{i}\Omega(\hat{A}_0 - \hat{A}_2)\right]. \quad (2.31)$$

If the plate is sufficiently far above the wall for the isolated plate results in (2.25)–(2.27) to be appropriate, the coefficients can be replaced by their analytical forms. After some algebra this leads to

$$\hat{p}(y_1, 0, y_3, \Omega) = -\frac{2\mathrm{i}\rho_0 \Gamma U_\infty}{\pi\Omega} \frac{h}{y_1^2 + h^2} \frac{\mathrm{e}^{-\Omega|b|/l}}{H_0^{(1)}(\Omega) + \mathrm{i}H_1^{(1)}(\Omega)} \quad \text{for} \quad \Omega > 0. \quad (2.32)$$

This approximate form for the Fourier transform of the pressure is plotted in figure 3 for comparison with the full solution. The agreement is surprisingly good even though $|y_1|$ and h are not particularly large.

This approximate expression for $\hat{p}(y_1, 0, y_3, \Omega)$ can be written compactly by noting that, since from (2.26)

$$\left.\begin{aligned} \hat{A}_0(\Omega) &= -\frac{4\mathrm{i}}{\pi\Omega} \frac{\mathrm{e}^{-\Omega|b|/l}}{H_0^{(1)}(\Omega) + \mathrm{i}H_1^{(1)}(\Omega)} \quad \text{for} \quad \Omega > 0, \\ \hat{p}(y_1, 0, y_3, \Omega) &= \tfrac{1}{2}\rho_0 \Gamma U_\infty \frac{h}{y_1^2 + h^2} \hat{A}_0(\Omega). \end{aligned}\right\} \quad (2.33)$$

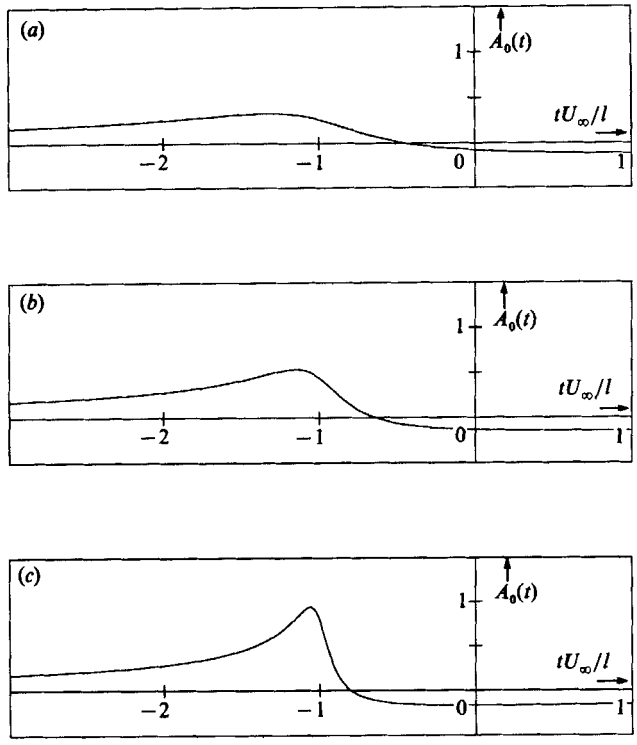

FIGURE 4. Plots of $A_0(t)$ for moderate or large h/l. (a) $b = 0.5l$, (b) $b = 0.25l$, (c) $b = 0.1l$.

The form of $\hat{A}_0(\Omega)$ is so simple that it is feasible to invert the Fourier transform to determine the time history of A_0:

$$A_0(t) = \frac{1}{2\pi}\int_{-\infty}^{\infty} \hat{A}_0(\Omega)\,\mathrm{e}^{-\mathrm{i}\Omega t U_\infty/l}\,\mathrm{d}\Omega = \frac{1}{\pi}\int_0^{\infty}\left[\cos\left(\frac{\Omega t U_\infty}{l}\right)\mathrm{Re}\,\hat{A}_0(\Omega) + \sin\left(\frac{\Omega t U_\infty}{l}\right)\mathrm{Im}\,\hat{A}_0(\Omega)\right]\mathrm{d}\Omega, \quad (2.34)$$

where we have used the fact that $\hat{A}_0(-\Omega)$ is the complex conjugate of $\hat{A}_0(\Omega)$. For $\Omega > 0$, $\hat{A}_0(\Omega)$ is given in (2.26). The integral was evaluated numerically for three values of b and the results are shown in figure 4. Inversion of (2.33) leads to

$$p(y_1, 0, y_3, t) = \tfrac{1}{2}\rho_0 \Gamma U_\infty \frac{h}{y_1^2 + h^2} A_0(t). \quad (2.35)$$

The pressure perturbation evidently has the same phase all along the wall. We see from figure 4 that this pressure disturbance reaches its maximum just before $t = -l/U_\infty$, which is the time the vortex passes the leading edge of the plate.

The function $A_0(t)$ is seen to be of order unity, and a comparison of the pressure with and without (see (2.10)) a LEBU shows that the near-field incompressible fluctuations are increased by a factor $U_\infty h/\Gamma$. The incident vortex produces unsteady flow velocities of the order of Γ/h and, since it models low-intensity turbulence, this is much smaller than the free-stream velocity U_∞. The presence of the LEBU therefore leads to a considerable enhancement of the near-field pressures. In the next section we shall investigate how the acoustic far field is affected.

3. The outer acoustic flow field

The effects of compressibility become important at large distances from the vortex and the LEBU. In this section we shall calculate the pressure fluctuations in this acoustic field. The vorticity distribution was determined in §2 and it is convenient to use a theory of sound generation that places emphasis on vorticity as an acoustic source. Howe (1975) has shown that, in a low-Mach-number flow with uniform and constant entropy, the equations of fluid motion reduce to

$$\left(\frac{1}{c^2}\frac{\partial^2}{\partial\tau^2}-\nabla^2\right)B = \operatorname{div}(\boldsymbol{\omega}\times\boldsymbol{v}), \tag{3.1}$$

where c is the speed of sound. The variable B is defined by

$$B = \int \mathrm{d}p/\rho + \tfrac{1}{2}v^2 \tag{3.2}$$

and outside vortical regions reduces to

$$B = -\frac{\partial\phi}{\partial t}. \tag{3.3}$$

In the acoustic far field, linearization shows that

$$B' = \frac{p'}{\rho_0}, \tag{3.4}$$

for a low-Mach-number flow.

In order to solve (3.1) we introduce a Green function $G(\boldsymbol{y},\tau\,|\,\boldsymbol{x},t)$ defined by

$$\left(\frac{1}{c^2}\frac{\partial^2}{\partial\tau^2}-\nabla^2\right)G = \delta(\boldsymbol{y}-\boldsymbol{x},t-\tau) \quad \text{in} \quad y_2>0 \tag{3.5}$$

together with $\partial G/\partial y_2 = 0$ on $y_2 = 0$ and a radiation condition at infinity. This is the familiar half-space Green function:

$$G(\boldsymbol{y},\tau\,|\,\boldsymbol{x},t) = \frac{\delta(t-\tau-|\boldsymbol{x}-\boldsymbol{y}|/c)}{4\pi|\boldsymbol{x}-\boldsymbol{y}|}+\frac{\delta(t-\tau-|\boldsymbol{x}-\boldsymbol{y}^*|/c)}{4\pi|\boldsymbol{x}-\boldsymbol{y}^*|}. \tag{3.6}$$

$\boldsymbol{y}^*$ is the image of the point $\boldsymbol{y}$ in the surface $y_2 = 0$, $\boldsymbol{y}^* = (y_1, -y_2, y_3)$. For a position $\boldsymbol{x}$ in the far field, where $R = (x_1^2+x_2^2)^{\frac{1}{2}}$ is large in comparison with $(y_1^2+y_2^2)^{\frac{1}{2}}$, G reduces to

$$G(\boldsymbol{y},\tau\,|\,\boldsymbol{x},t) = \frac{1}{4\pi r}\left[\delta\left(t-\tau-\frac{r}{c}+\frac{x_\alpha y_\alpha}{rc}\right)+\delta\left(t-\tau-\frac{r}{c}+\frac{x_\alpha y_\alpha^*}{rc}\right)\right], \tag{3.7}$$

with $r = |\boldsymbol{x}-y_3\boldsymbol{k}|$. The repeated suffix α is summed over 1 and 2. When the source is compact in the y_1 and y_2 directions, the argument of the δ-functions can be expanded as Taylor series. The first three terms in this expansion yield

$$G(\boldsymbol{y},\tau\,|\,\boldsymbol{x},t) = \frac{1}{2\pi r}\left[\delta\left(t-\tau-\frac{r}{c}\right)+\frac{x_1 y_1}{rc}\dot{\delta}\left(t-\tau-\frac{r}{c}\right)+\frac{x_1^2y_1^2+x_2^2y_2^2}{2r^2c^2}\ddot{\delta}\left(t-\tau-\frac{r}{c}\right)+\ldots\right]. \tag{3.8}$$

A straightforward algebraic rearrangement shows that

$$B\left(\frac{1}{c^2}\frac{\partial^2}{\partial\tau^2}-\nabla^2\right)G-G\left(\frac{1}{c^2}\frac{\partial^2}{\partial\tau^2}-\nabla^2\right)B = \frac{1}{c^2}\frac{\partial}{\partial\tau}\left(B\frac{\partial G}{\partial\tau}-G\frac{\partial B}{\partial\tau}\right)-\boldsymbol{\nabla}\cdot(B\boldsymbol{\nabla}G-G\boldsymbol{\nabla}B). \tag{3.9}$$

Equations (3.1) and (3.5) may be used to simplify the left-hand side of this identity to give

$$B\delta(\boldsymbol{x}-\boldsymbol{y},t-\tau)-G\boldsymbol{\nabla}\cdot(\boldsymbol{\omega}\times\boldsymbol{v})=\frac{1}{c^2}\frac{\partial}{\partial\tau}\left(B\frac{\partial G}{\partial\tau}-G\frac{\partial B}{\partial\tau}\right)-\boldsymbol{\nabla}\cdot(B\boldsymbol{\nabla}G-G\boldsymbol{\nabla}B). \quad (3.10)$$

When there is a LEBU we shall surround it by a fixed control surface S with normal $\boldsymbol{n}$, as shown in figure 2. Then integration of (3.10) over the region external to S in $y_2 \geqslant 0$ and over all times leads to

$$B(\boldsymbol{x},t)=-\int\boldsymbol{\nabla}G\cdot(\boldsymbol{\omega}\times\boldsymbol{v})\,\mathrm{d}^3\boldsymbol{y}\,\mathrm{d}\tau-\int_S B\frac{\partial G}{\partial n}\mathrm{d}S\,\mathrm{d}\tau. \quad (3.11)$$

We have used the fact that $\partial G/\partial n$ vanishes on $y_2=0$ and that, since the surfaces are rigid, $\partial B/\partial n$ is zero both on the LEBU surface S and on the plane wall $y_2=0$.

In our two-dimensional model problem, the vorticity is only in the y_3 direction, $\boldsymbol{\omega}=\omega_3\boldsymbol{k}$. After substitution for G from (3.8), the δ-functions can be used to evaluate the τ-integrals. We then find that in the far field

$$B(\boldsymbol{x},t)=\frac{x_1}{2\pi c}\frac{\partial}{\partial t}\int\frac{[v_2\,\omega_3]}{r^2}\mathrm{d}^3\boldsymbol{y}+\frac{1}{2\pi c^2}\frac{\partial^2}{\partial t^2}\int\frac{[(x_1^2y_1v_2-x_2^2y_2v_1)\,\omega_3]}{r^3}\mathrm{d}^3\boldsymbol{y}$$
$$-\frac{x_1}{2\pi c}\frac{\partial}{\partial t}\int_S\frac{[n_1B]}{r^2}\mathrm{d}S-\frac{1}{2\pi c^2}\frac{\partial^2}{\partial t^2}\int_S\frac{[(x_1^2y_1n_1+x_2^2y_2n_2)\,B]}{r^3}\mathrm{d}S, \quad (3.12)$$

where the square brackets denote that the function they enclose is to be evaluated at retarded time $t-r/c$, with $r=|\boldsymbol{x}-y_3\boldsymbol{k}|$.

Finally (3.3) and (3.4) may be used to rewrite B in terms of the velocity potential on S and in terms of the distant pressure perturbation in the far field. This leads to

$$p'(\boldsymbol{x},t)=\frac{\rho_0x_1}{2\pi c}\frac{\partial}{\partial t}\int\frac{[v_2\,\omega_3]}{r^2}\mathrm{d}^3\boldsymbol{y}+\frac{\rho_0}{2\pi c^2}\frac{\partial^2}{\partial t^2}\int\frac{[(x_1^2y_1v_2-x_2^2y_2v_1)\,\omega_3]}{r^3}\mathrm{d}^3\boldsymbol{y}$$
$$+\frac{\rho_0x_1}{2\pi c}\frac{\partial^2}{\partial t^2}\int_S\frac{[n_1\phi]}{r^2}\mathrm{d}S+\frac{\rho_0}{2\pi c^2}\frac{\partial^3}{\partial t^3}\int_S\frac{[(x_1^2y_1n_1+x_2^2y_2n_2)\,\phi]}{r^3}\mathrm{d}S. \quad (3.13)$$

Sources of sound are concentrated in the vortical regions and on the surface of the LEBU. At low Mach numbers the flow in this inner region is incompressible and has been calculated in §2.

3.1. *In the absence of a LEBU*

When there is no turbulence manipulator, the expression for the distant pressure in (3.13) simplies to just the volume integrals:

$$p'(\boldsymbol{x},t)=\frac{\rho_0x_1}{2\pi c}\frac{\partial}{\partial t}\int\frac{[v_2\,\omega_3]}{r^2}\mathrm{d}^3\boldsymbol{y}+\frac{\rho_0}{2\pi c^2}\frac{\partial^2}{\partial t^2}\int\frac{[(x_1^2y_1v_2-x_2^2y_2v_1)\,\omega_3]}{r^3}\mathrm{d}^3\boldsymbol{y}. \quad (3.14)$$

In this case the vorticity distribution is given by (2.1). It is only non-zero within the vortex core. The form for the velocity field $\boldsymbol{v}$ within the core is given by (2.4) and straightforward integration shows that

$$\int v_2\,\omega_3\,\mathrm{d}y_1\,\mathrm{d}y_2=0,$$

$$\int y_1v_2\,\omega_3\,\mathrm{d}y_1\,\mathrm{d}y_2=\frac{\Gamma^2}{8\pi}(1+\epsilon\cos\tfrac{1}{2}\omega t)$$

and

$$\int y_2v_1\,\omega_3\,\mathrm{d}y_1\,\mathrm{d}y_2=-\frac{\Gamma^2}{8\pi}(1-\epsilon\cos\tfrac{1}{2}\omega t).$$

The far-field pressure in (3.14) is therefore equal to

$$p'(\boldsymbol{x},t) = -\frac{\rho_0 \epsilon \Gamma^2 \omega^2}{64\pi^2 c^2}(x_1^2 - x_2^2)\int_{-\infty}^{\infty} \frac{\cos\left[\frac{1}{2}\omega(t-r/c)\right]}{r^3}\,\mathrm{d}y_3. \tag{3.15}$$

For large $\omega R/c$, where $R = (x_1^2 + x_2^2)^{\frac{1}{2}}$, the y_3 integral may be evaluated by the method of stationary phase and we finally obtain

$$p'(\boldsymbol{x},t) = -\frac{\rho_0 \epsilon \Gamma^2}{32 R^{\frac{1}{2}}}\left(\frac{\omega}{\pi c}\right)^{\frac{3}{2}} \frac{x_1^2 - x_2^2}{R^2} \cos\left[\tfrac{1}{2}\omega\left(t - \frac{R}{c}\right) - \tfrac{1}{4}\pi\right]. \tag{3.16}$$

This form for the pressure prturbation is typical of that due to two-dimensional quadrupoles. It decays with the inverse-square-root of distance from the source and has a directivity described by $(x_1^2 - x_2^2)/R^2$. Note that the pressure perturbation is proportional to ϵ: the vortex only generates sound owing to its eccentricity.

Howe (1975) determined the acoustical field of an elliptical vortex in free space. He found that it was equivalent to that produced by rotating quadrupoles. Equation (3.16) can be recovered from Howe's result by a superposition of the field of an isolated vortex with that due to image quadrupoles in the hard wall.

3.2. *With a LEBU*

The acoustic field generated as the vortex passes over a LEBU is described by (3.13), with $\boldsymbol{\omega}$, $\boldsymbol{v}$ and ϕ as given in (2.13)–(2.16). The pressure perturbation may be conveniently decomposed into dipole and quadrupole fields, denoted by $p'_{\mathrm{d}}(\boldsymbol{x},t)$ and $p'_{\mathrm{q}}(\boldsymbol{x},t)$ respectively, with

$$p'_{\mathrm{d}}(\boldsymbol{x},t) = \frac{\rho_0 x_1}{2\pi c}\left\{\frac{\partial}{\partial t}\int \frac{[v_2\omega_3]}{r^2}\,\mathrm{d}^3\boldsymbol{y} + \frac{\partial^2}{\partial t^2}\int_S \frac{[n_1\phi]}{r^2}\,\mathrm{d}S\right\} \tag{3.17}$$

and

$$p'_{\mathrm{q}}(\boldsymbol{x},t) = \frac{\rho_0}{2\pi c^2}\left\{\frac{\partial^2}{\partial t^2}\int \frac{[(x_1^2 y_1 v_2 - x_2^2 y_2 v_1)\omega_3]}{r^3}\,\mathrm{d}^3\boldsymbol{y} + \frac{\partial^3}{\partial t^3}\int_S \frac{[(x_1^2 y_1 n_1 + x_2^2 y_2 n_2)\phi]}{r^3}\,\mathrm{d}S\right\}. \tag{3.18}$$

As before $r = |\boldsymbol{x} - y_3\boldsymbol{k}|$ and the square brackets denote that the function they enclose is to be evaluated at retarded time $t - r/c$. In the absence of a LEBU, we found the vortex sound to be quadrupole. The introduction of the LEBU leads to new dipole sources.

The integrals in (3.17) are evaluated in Appendix B, where it is shown that the strength of the dipole is proportional to $A_0^2(t)$ ($A_0(t)$ is the coefficient of the singular term in the Glauert series). This leads to a sound field

$$p'_{\mathrm{d}}(\boldsymbol{x},t) = \frac{\rho_0 x_1 \Gamma^2}{16 c l}\frac{\partial}{\partial t}\int \frac{A_0^2(t - r/c)}{r^2}\,\mathrm{d}y_3. \tag{3.19}$$

This dipole sound field is proportional to Γ^2, that is it depends on the square of the velocity fluctuations induced by the vortex. For a vortex producing weak velocity fluctuations Γ is small, and the Glauert coefficient, $A_0(t)$, in (3.19) can be evaluated from the linear theory in §2.

We now turn our attention to the quadrupole sound in (3.18), but since we already have a second-order dipole we shall only evaluate the quadrupole source strength to

first order in Γ. The integrals are again evaluated in Appendix B, where we find that the quadrupole is in the 2–2 direction, with an associated pressure field

$$p'_{\mathrm{q}}(\boldsymbol{x},t) = \frac{\rho_0 x_2^2 h}{2\pi c^2}\frac{\partial^2}{\partial t^2}\int_{-\infty}^{\infty}\frac{\mathrm{d}y_3}{r^3}\int_{-l}^{l}(g(y_1,t-r/c)+U_\infty f(y_1,t-r/c))\,\mathrm{d}y_1. \tag{3.20}$$

The function $g(y_1,t)$ is defined in (2.19).

When the dipole and quadrupole contributions in (3.19) and (3.20) respectively are collected together they lead to a distant pressure perturbation of the form

$$\begin{aligned} p'(\boldsymbol{x},t) = {} & \frac{\rho_0 x_1 \Gamma^2}{16cl}\frac{\partial}{\partial t}\int_{-\infty}^{\infty}\frac{A_0^2(t-r/c)}{r^2}\mathrm{d}y_3 \\ & + \frac{\rho_0 x_2^2 h}{2\pi c^2}\frac{\partial^2}{\partial t^2}\int_{-\infty}^{\infty}\frac{\mathrm{d}y_3}{r^3}\int_{-l}^{l}(g(y_1,t-r/c)+U_\infty f(y_1,t-r/c))\,\mathrm{d}y_1. \end{aligned} \tag{3.21}$$

This expression has a simple physical interpretation. It is shown in Appendix C that the plate exerts a thrust $\rho_0\pi\Gamma^2A_0^2(t)/8l$ per unit spanwise length on the fluid. The dipole term in (3.21) describes the acoustic field generated by this unsteady streamwise force. In addition there is a linear lift force in the 2-direction of strength

$$\rho_0\int_{-l}^{l}\{g(y_1,t)+U_\infty f(y_1,t)\}\,\mathrm{d}y_1$$

per unit spanwise length. In free space this lift produces a dipole sound field (Howe 1976). But here the image of this normal force in the adjacent plane surface is equal and opposite and together they lead to the quadrupole term in (3.21).

The y_1 integral in (3.21) was evaluated in §2 (see (2.29)–(2.33)). In particular it was shown that, if the LEBU is sufficiently far above the plane wall for the flow in the vicinity of the plate to be uninfluenced by images in the wall,

$$\int_{-l}^{l}\{g(y_1,t)+U_\infty f(y_1,t)\}\,\mathrm{d}y_1 = -\tfrac{1}{2}\pi\Gamma U_\infty A_0(t). \tag{3.22}$$

When this relationship is used in (3.21), the expression for the distant pressure perturbation simplifies to

$$p'(\boldsymbol{x},t) = \frac{\rho_0 x_1 \Gamma^2}{16cl}\frac{\partial}{\partial t}\int\frac{A_0^2(t-r/c)}{r^2}\mathrm{d}y_3 - \frac{\rho_0 x_2^2 \Gamma h U_\infty}{4c^2}\frac{\partial^2}{\partial t^2}\int\frac{A_0(t-r/c)}{r^3}\mathrm{d}y_3. \tag{3.23}$$

$A_0(t)$ has been plotted in figure 4. It is typically of order unity and varies over a timescale l/U_∞. The quadrupole term in (3.23) therefore leads to pressure fluctuations that are a factor $MU_\infty h/\Gamma$ smaller than those induced by the dipole. Since the mean flow Mach number is very low in underwater applications, this factor is small. Moreover, the quadrupole sound vanishes identically on the surface of particular interest, $x_2 = 0$. The distant pressure field is therefore dominated by the dipole term in (3.23):

$$p'(\boldsymbol{x},t) \approx \frac{\rho_0 x_1 \Gamma^2}{16cl}\int\frac{1}{r^2}\frac{\partial}{\partial t}A_0^2(t-r/c)\,\mathrm{d}y_3. \tag{3.24}$$

The contribution to the sound field from unit spanwise length of LEBU is proportional to $\mathrm{d}A_0^2/\mathrm{d}t$. For moderate and large values of h, $A_0(t)$ has the form given by (2.26) and (2.34) and the derivative $\mathrm{d}A_0^2(t)/\mathrm{d}t$ is plotted in figure 5. This source strength becomes intense for small values of b (the perpendicular distance between the LEBU and the axis of the vortex at time $t = 0$).

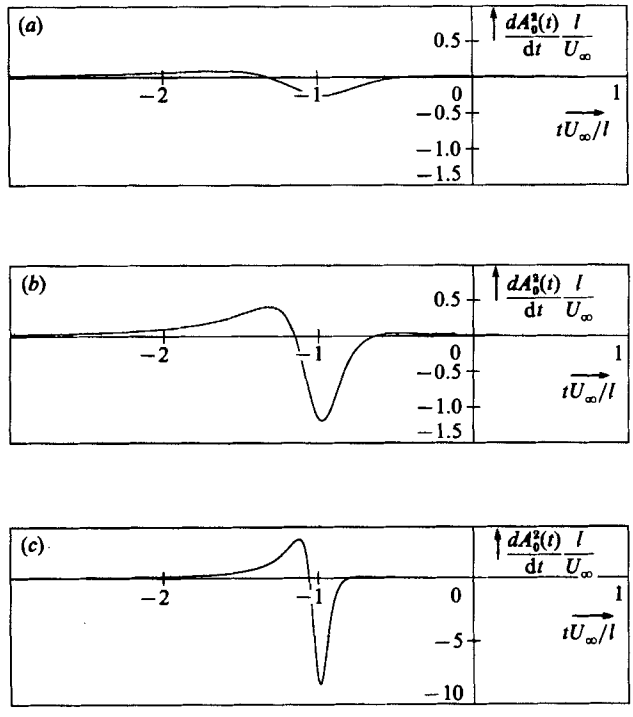

FIGURE 5. Plots of $dA_0^2(t)/dt$ for moderate or large h/l. (*a*) $b = 0.5l$, (*b*) $b = 0.25l$, (*c*) $b = 0.1l$.

The y_3 integral in (3.24) may be rewritten using the technique introduced by Ffowcs Williams (1969). First we change the integration variable from y_3 to the retarded time $\tau = t - r/c$ to obtain

$$p'(\boldsymbol{x},t) = \frac{\rho_0 x_1 \Gamma^2}{8c^2 l}\int_{-\infty}^{t-R/c} \frac{1}{((t-\tau)^2 - R^2/c^2)^{\frac{1}{2}}(t-\tau)}\frac{\mathrm{d}}{\mathrm{d}\tau}A_0^2(\tau)\,\mathrm{d}\tau, \tag{3.25}$$

with $R = (x_1^2 + x_2^2)^{\frac{1}{2}}$. The integrand evidently has an integrable singularity at $\tau = t - R/c$. Following Ffowcs Williams (1969), we expand the other terms in the denominator of the integrand about this value of τ. This procedure shows that, for large R,

$$p'(\boldsymbol{x},t) = \frac{\rho_0 x_1 \Gamma^2}{8l(2cR^3)^{\frac{1}{2}}}\int_{-\infty}^{t-R/c} \frac{1}{(t-\tau-R/c)^{\frac{1}{2}}}\frac{\mathrm{d}}{\mathrm{d}\tau}A_0^2(\tau)\,\mathrm{d}\tau. \tag{3.26}$$

The integral has been evaluated numerically and the function

$$\left(\frac{l}{U_\infty}\right)^{\frac{1}{2}}\int_{-\infty}^{t} \frac{1}{(t-\tau)^{\frac{1}{2}}}\frac{\mathrm{d}}{\mathrm{d}\tau}A_0^2(\tau)\,\mathrm{d}\tau$$

is plotted in figure 6 for discrete values of t. The graphs show that this non-dimensional function is of order unity. It varies rapidly and has its maximum magnitude at times near $t = -l/U_\infty$, the time at which the vortex passes the leading edge of the LEBU. We see then from (3.26) that $p'(\boldsymbol{x},t)$ is significant for times in the range $R/c - 2l/U_\infty$ to R/c and that it is then of order

$$\tfrac{1}{8}\rho_0 |x_1| \Gamma^2 \left(\frac{M}{2R^3 l^3}\right)^{\frac{1}{2}}. \tag{3.27}$$

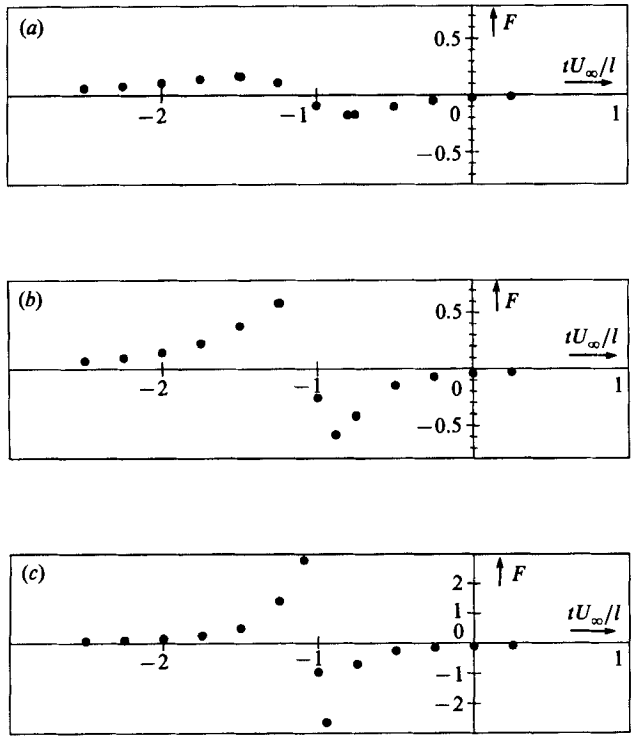

FIGURE 6. Plots of

$$F = \left(\frac{l}{U_\infty}\right)^{\frac{1}{3}} \int_{-\infty}^{t} \frac{1}{(t-\tau)^{\frac{1}{3}}} \frac{\mathrm{d}}{\mathrm{d}\tau} A_0^2(\tau)\,\mathrm{d}\tau$$

for moderate or large h/l. (a) $b = 0.5l$, (b) $b = 0.25l$, (c) $b = 0.1l$.

It is interesting to compare the distant pressure perturbation with and without the LEBU. It is apparent from (3.16) that in the absence of a LEBU, the far-field pressure is proportional to the small eccentricity, ϵ, of the vortex core. All vortical elements satisfying Taylor's hypothesis are silent. When the vortex is convected past a LEBU even vorticity that convects without change generates sound as it exerts an unsteady suction on the plate. A comparison of (3.16) and (3.27) shows that the LEBU enhances the distant pressure field by a factor $\epsilon^{-1}M^{-1}(\omega l/U_\infty)^{-3}$. Since both ϵ and M are small this represents a considerable augmentation in the sound of a single eddy.

4. A LEBU in a turbulent boundary layer

The sound field produced by the convection of an idealized two-dimensional eddy past a LEBU was evaluated in §3. The exact solution of this simplified problem highlights the main noise source mechanism, and the physical insight obtained will now be applied to sound generation in a three-dimensional turbulent layer modified by a LEBU.

Consider a LEBU of chord $2l$ and span $2L$, positioned at a height h above the rigid wall $x_2 = 0$. Again we enclose the LEBU by a control surface S. The half-space Green

function $G(\boldsymbol{y},\tau\,|\,\boldsymbol{x},t)$ in (3.6) may be used to write down a solution of the Ffowcs Williams–Hawkings equation (Ffowcs Williams & Hawkings 1969, equation (2.8)) to give

$$c^2\rho'(\boldsymbol{x},t) = \int \frac{\partial^2 G}{\partial y_i \partial y_j} T_{ij}\,\mathrm{d}^3\boldsymbol{y}\,\mathrm{d}\tau - \int_S \frac{\partial G}{\partial y_i} p n_i\,\mathrm{d}S\,\mathrm{d}\tau. \tag{4.1}$$

Lighthill's quadrupole source T_{ij} simplifies to $\rho v_i v_j + (p' - c^2\rho')\,\delta_{ij}$ in an inviscid fluid. ρ' denotes the density perturbation and is equal to p'/c^2 in an isentropic fluid in linear motion. The volume integral is to be taken over the positive y_2 half-space external to the surface S. The fact that the normal component of velocity vanishes both on the plane $y_2 = 0$ and on the surface of the LEBU has been used in deriving (4.1).

The observer's position $\boldsymbol{x}$ will be taken to be in the far field, many chord lengths away from the LEBU, so that $|\boldsymbol{x}|$ is large in comparison with both the wavelength and $(y_1^2+y_2^2)^{\frac{1}{2}}$ as $\boldsymbol{y}$ varies over the surface of the LEBU. $|\boldsymbol{x}|$ is not necessarily large in comparison with L, because the span of the LEBU may be considerable.

Differentiation of the expansion for $G(\boldsymbol{y},\tau\,|\,\boldsymbol{x},t)$ in (3.8) shows that

$$\frac{\partial G}{\partial y_1} = \frac{x_1}{2\pi r^2 c}\dot{\delta}\left(t-\tau-\frac{r}{c}\right), \quad \frac{\partial G}{\partial y_3} = \frac{x_3-y_3}{2\pi r^2 c}\dot{\delta}\left(t-\tau-\frac{r}{c}\right),$$

while

$$\frac{\partial G}{\partial y_2} = \frac{x_2^2 y_2}{2\pi r^3 c^2}\ddot{\delta}\left(t-\tau-\frac{r}{c}\right),$$

with again $r = |\boldsymbol{x}-y_3\boldsymbol{k}|$. After substitution for the derivatives of $\boldsymbol{G}(\boldsymbol{y},\tau\,|\,\boldsymbol{x},t)$ in (4.1), we find the dipole term in the distant pressure field to be

$$p'_{\mathrm{d}}(\boldsymbol{x},t) = -\frac{\partial}{\partial t}\int \frac{(x_1 n_1 + (x_3-y_3)\,n_3)}{2\pi r^2 c}\,p(\boldsymbol{y},t-r/c)\,\mathrm{d}S. \tag{4.2}$$

The dipole sound field evidently depends on the 1- and 3-components of the force exerted on the fluid by the LEBU. The surface normal component n_3 is only non-zero at the cross-stream edges of the LEBU and so the 3-component of the force is small. Although n_1 is only non-zero at the leading and trailing edges of the plate, the pressure at the leading edge is singular and even an infinitesimally thin plate exerts a thrust on the fluid. This leads to the main dipole sound. It is shown in Appendix C that the thrust per unit spanwise length is proportional to the square of the velocity fluctuations. We will denote the thrust/spanwise length of LEBU by $F(y_3,t)$. Substitution for the force in (4.2) shows that

$$p'_{\mathrm{d}}(\boldsymbol{x},t) = \frac{x_1}{2\pi c}\frac{\partial}{\partial t}\int_{-L}^{L} \frac{F(y_3,t-r/c)}{r^2}\,\mathrm{d}y_3. \tag{4.3}$$

Let $\tilde{p}_{\mathrm{d}}(\boldsymbol{x},\omega)$ denote the Fourier transform of this dipole pressure field:

$$\tilde{p}_{\mathrm{d}}(\boldsymbol{x},\omega) = \int p'_{\mathrm{d}}(\boldsymbol{x},t)\,\mathrm{e}^{\mathrm{i}\omega t}\,\mathrm{d}t. \tag{4.4}$$

The Fourier transform of (4.3) gives

$$\tilde{p}_{\mathrm{d}}(\boldsymbol{x},\omega) = -\frac{\mathrm{i}\omega x_1}{2\pi c}\int_{-L}^{L} \frac{\tilde{F}(y_3,\omega)}{r^2}\,\mathrm{e}^{\mathrm{i}\omega r/c}\,\mathrm{d}y_3, \tag{4.5}$$

and this can be used to calculate the power spectral density of the dipole pressure field, $P_{\mathrm{d}}(\boldsymbol{x},\omega)$.

For statistically stationary turbulence

$$P_{\mathrm{d}}(\boldsymbol{x},\omega)=\frac{1}{2\pi}\int\overline{\tilde{p}_{\mathrm{d}}(\boldsymbol{x},\omega)\,\tilde{p}_{\mathrm{d}}(\boldsymbol{x},\omega')}\,\mathrm{d}\omega', \tag{4.6}$$

where the overbar denotes an ensemble average. After substitution from (4.5) this leads to

$$P_{\mathrm{d}}(\boldsymbol{x},\omega)=-\frac{\omega\omega'}{2\pi}\left(\frac{x_1}{2\pi c}\right)^2\int_{-L}^{L}\int_{-L}^{L}\frac{\overline{\tilde{F}(y_3,\omega)\,\tilde{F}(y_3',\omega')}}{r^2r'^2}\,\mathrm{e}^{\mathrm{i}(\omega r+\omega' r')/c}\,\mathrm{d}y_3\,\mathrm{d}y_3', \tag{4.7}$$

with $r'=|\boldsymbol{x}-y_3'\boldsymbol{k}|$. Now for statistically stationary turbulence

$$\overline{\tilde{F}(y_3,\omega)\,\tilde{F}(y_3+\xi,\omega')}=2\pi\mathscr{F}(y_3,\xi,\omega')\,\delta(\omega+\omega'), \tag{4.8}$$

where $\mathscr{F}(y_3,\xi,\omega')$ is the cross-power spectral density of $F(y_3,t)$;

$$\mathscr{F}(y_3,\xi,\omega')=\int\overline{F(y_3,t)\,F(y_3+\xi,t+\tau)}\,\mathrm{e}^{\mathrm{i}\omega'\tau}\,\mathrm{d}\tau. \tag{4.9}$$

The relationship in (4.8) shows that (4.7) reduces to

$$P_{\mathrm{d}}(\boldsymbol{x},\omega)=\left(\frac{\omega x_1}{2\pi c}\right)^2\int_{y_3=-L}^{L}\int_{\xi=-L-y_3}^{L-y_3}\frac{\mathscr{F}(y_3,\xi,-\omega)}{r^2r'^2}\,\mathrm{e}^{\mathrm{i}\omega(r-r')/c}\,\mathrm{d}\xi\,\mathrm{d}y_3. \tag{4.10}$$

An integral length scale, l_{I}, can be defined by

$$\int_{-\infty}^{\infty}\mathscr{F}(y_3,\xi,-\omega)\,\mathrm{d}\xi=l_{\mathrm{I}}\mathscr{F}(y_3,0,-\omega). \tag{4.11}$$

l_{I} is comparable in magnitude with the turbulent correlation lengthscale and, provided that it is small in comparison with both $2L$ and the wavelength $2\pi c/\omega$, (4.10) simplies to

$$P_{\mathrm{d}}(\boldsymbol{x},\omega)=\left(\frac{wx_1}{2\pi c}\right)^2\int_{-L}^{L}\frac{l_{\mathrm{I}}\mathscr{F}(y_3,0,-\omega)}{r^4}\mathrm{d}y_3. \tag{4.12}$$

When the turbulence is homogeneous, $\mathscr{F}(y_3,0,\omega)$ is virtually independent of y_3 along the length of the LEBU and $P_{\mathrm{d}}(\boldsymbol{x},\omega)$ becomes

$$P_{\mathrm{d}}(\boldsymbol{x},\omega)=\left(\frac{\omega x_1}{2\pi c}\right)_{l_{\mathrm{I}}}^2\mathscr{F}(0,0,-\omega)\int_{-L}^{L}\frac{\mathrm{d}y_3}{|\boldsymbol{x}-y_3\boldsymbol{k}|^4}. \tag{4.13}$$

The y_3 integral is of standard form (see Gradshteyn & Ryzhik 1980, p. 66) and we finally obtain

$$P_{\mathrm{d}}(\boldsymbol{x},\omega)=\left(\frac{\omega x_1}{2\pi c}\right)_{l_{\mathrm{I}}}^2\mathscr{F}(0,0,-\omega)\,I(\boldsymbol{x},L), \tag{4.14}$$

where

$$2R^3I(\boldsymbol{x},L)=\frac{R(L-x_3)}{R^2+(L-x_3)^2}+\frac{R(L+x_3)}{R^2+(L+x_3)^2}+\tan^{-1}\left(\frac{L-x_3}{R}\right)+\tan^{-1}\left(\frac{L+x_3}{R}\right), \tag{4.15}$$

with, as before, $R=(x_1^2+x_2^2)^{\frac{1}{2}}$.

If L is small in comparison with $|\boldsymbol{x}|$, $I(\boldsymbol{x},L)$ simplies to $2L/|\boldsymbol{x}|^4$. But when $L=R$ and $x_3=0$,

$$I(\boldsymbol{x},L)=\frac{L}{|\boldsymbol{x}|^4}(\tfrac{1}{2}+\tfrac{1}{4}\pi). \tag{4.16}$$

On the other hand, for L large in comparison with $|\boldsymbol{x}|$,

$$I(\boldsymbol{x}, L) = \frac{\pi}{2R^3}. \tag{4.17}$$

We can combine all these forms for $I(\boldsymbol{x}, L)$ together with (4.14) to give

$$P_{\mathrm{d}}(\boldsymbol{x}, \omega) \sim \left(\frac{\omega}{2\pi c}\right)^2 \frac{l_{\mathrm{I}}}{|\boldsymbol{x}|^2} \min(L, |\boldsymbol{x}|)\, \mathscr{F}(0, 0, -\omega). \tag{4.18}$$

When the function $\mathscr{F}(0, 0, -\omega)$ is rewritten in non-dimensional form we finally obtain

$$P_{\mathrm{d}}(\boldsymbol{x}, \omega) \sim \left(\frac{\rho_0 u_\tau^2 \omega l}{2\pi c}\right)^2 \frac{l_{\mathrm{I}} l}{U_{\mathrm{c}} |\boldsymbol{x}|^2} \min(L, |\boldsymbol{x}|)\, \Phi_{\mathrm{d}}\left(\frac{\omega l}{U_{\mathrm{c}}}\right), \tag{4.19}$$

where velocity fluctuations have been non-dimensionalized with respect to the friction velocity, u_τ, and U_{c} is a typical eddy convection velocity.

$$\Phi_{\mathrm{d}}\left(\frac{\omega l}{U_{\mathrm{c}}}\right) = \frac{U_{\mathrm{c}}}{\rho_0^2 u_\tau^4 l^3} \mathscr{F}(0, 0, -\omega), \tag{4.20}$$

which becomes

$$\Phi_{\mathrm{d}}\left(\frac{\omega l}{U_{\mathrm{c}}}\right) = \frac{1}{(\rho_0 u_\tau^2 l)^2} \int \overline{F(y_3, t) F(y_3, t+\tau)}\, \mathrm{e}^{-\mathrm{i}\omega\tau} \frac{U_{\mathrm{c}}\, \mathrm{d}\tau}{l} \tag{4.21}$$

once (4.9) has been used to express $\mathscr{F}(0, 0, -\omega)$ in terms of $F(y_3, t)$. The calculation of $F(y_3, t)$ in Appendix C and the plots in figure 4 show $F(y_3, t)$ to vary over a timescale l/U_{c} and to be of order $\rho_0 u^2 l$, where u is a typical velocity fluctuation. $\Phi_{\mathrm{d}}(\omega l/U_{\mathrm{c}})$ is therefore of the same order as the non-dimensional power spectral density of the function u^2/u_τ^2.

The pressure spectrum of the dipole sound on the hard surface, $x_2 = 0$, is caused by centred waves travelling over the surface from the LEBU with the sound speed. It scales in the way indicated in (4.19) and, in particular, decays with distance from the LEBU.

A transducer mounted on the rigid surface $x_2 = 0$ would detect the noise of the turbulent quadrupole sources, T_{ij} in equation (4.1), in addition to this centred dipole field. These quadrupoles are distributed throughout the boundary layer and generate sound whether or not a LEBU is present. Their sound field has been investigated in detail by Ffowcs Williams (1965, 1982). In particular the mean square of the quadrupole source strength is found to be proportional to the fourth power of the velocity fluctuations. The experiments of Westphal (1986), Bonnet *et al.* (1987), Coustols *et al.* (1987) and others have shown that these velocity fluctuations are significantly reduced by the introduction of a LEBU. In order to highlight this attenuation we shall follow these experimenters and scale the velocity fluctuations on u_τ, which has a peak reduction of between 8 and 23% downstream of a LEBU. We found in (4.19) that the distant surface pressure perturbation induced by the LEBU consists only of disturbances travelling over the surface with the sound speed. The installation of LEBUs therefore introduces no additional pressure fluctuations with supersonic wavenumbers and, for these spectral components, we can expect a reduction in flow noise due to the reduction in the strength of the turbulent sources, T_{ij}.

The installation of the LEBU increases the surface pressure spectrum for spectral elements with sonic phase speeds. To see whether the net effect of introducing

LEBUs is beneficial, we shall compare the dipole field in (4.19) with the flow noise at the acoustic wavenumber in the absence of LEBUs. Ffowcs Williams (1965) found that the surface pressure spectrum under a boundary layer of finite extent has a non-integrable singularity for spectral elements with sonic phase speeds. This singularity was analysed by Bergeron (1973) who showed that it arises due to a form of Olbers' paradox, because the turbulent source region is considered to be of infinite extent and the sound field from each source element does not decrease rapidly enough with distance for the integrated effect to be finite. He demonstrated that when the source region has finite extent, D, the pressure spectrum is still singular but that the singularity is integrable. The strength of this singular field is given in a particularly convenient form by Ffowcs Williams (1982, equation (4.18)). Using his result, with the minor amendment discussed by Howe (1987), we find that the cross-power spectral density of the quadrupole surface pressure is given by

$$P_{\mathrm{q}}(k_1, k_3, \omega) = \frac{\rho_0^2 u_\tau^4 \omega^4 \Delta^7}{U_{\mathrm{c}} c^4} \ln\left(\frac{8\omega D}{\pi c}\right) \delta\left((\Delta k_1)^2 + (\Delta k_2)^2 - \left(\frac{\omega\Delta}{c}\right)^2\right) \Phi_{\mathrm{q}}\left(\frac{\omega\Delta}{U_{\mathrm{c}}}\right), \quad (4.22)$$

where Δ is the boundary-layer thickness. $\Phi_{\mathrm{q}}(\omega\Delta/U_{\mathrm{c}})$ is a non-dimensional function arising from the power spectral density of T_{ij} non-dimensionalized on u_τ.

The power spectral density of the surface pressure can be determined by an integration of (4.22) over wavenumber:

$$P_{\mathrm{q}}(\omega) = \frac{1}{(2\pi)^2} \int P_{\mathrm{q}}(k_1, k_2, \omega)\, \mathrm{d}k_1\, \mathrm{d}k_2. \quad (4.23)$$

The δ-function makes this integration straightforward and we obtain

$$P_{\mathrm{q}}(\omega) = \left(\frac{\rho_0 u_\tau^2 \omega^2 \Delta^2}{c^2}\right)^2 \frac{\Delta}{4\pi U_{\mathrm{c}}} \ln\left(\frac{8\omega D}{\pi c}\right) \Phi_{\mathrm{q}}\left(\frac{\omega\Delta}{U_{\mathrm{c}}}\right). \quad (4.24)$$

Sevik (1986) presents data which describe the functional form of $\Phi_{\mathrm{q}}(\omega\Delta/U_{\mathrm{c}})$. However this does not help us here because we wish to compare (4.24) with the dipole field in (4.19) and we have no data on the variation of $\Phi_{\mathrm{d}}(\omega l/U_{\mathrm{c}})$ with frequency. However a detailed study of Ffowcs Williams (1982) shows that

$$\Phi_{\mathrm{q}}\left(\frac{\omega\Delta}{U_{\mathrm{c}}}\right) = \frac{\pi}{8} \frac{V_{\mathrm{I}}}{\Delta^3} \frac{1}{\rho_0^2 u_\tau^4} \int \overline{(2T_{\alpha\beta}(\boldsymbol{y}, t)\, T_{\alpha\beta}(\boldsymbol{y}, t+\tau) + T_{\alpha\alpha}(\boldsymbol{y}, t)\, T_{\beta\beta}(\boldsymbol{y}, t+\tau))} \mathrm{e}^{-\mathrm{i}\omega\tau} \frac{U_{\mathrm{c}}\, \mathrm{d}\tau}{\Delta} \frac{\mathrm{d}y_2}{\Delta}, \quad (4.25)$$

where V_{I} is the integral correlation volume and α and β are summed over 1 and 3. In a low-Mach-number flow, the quadrupole source $T_{\alpha\beta}$ reduces to the Reynolds stress $\rho_0 u_\alpha u_\beta$ and $\Phi_{\mathrm{q}}(\omega\Delta/U_{\mathrm{c}})$ depends on the power spectral density of the non-dimensional functions $u_\alpha u_\beta/u_\tau^2$ and u^2/u_τ^2. We saw in (4.21) that $\Phi_{\mathrm{d}}(\omega l/U_{\mathrm{c}})$ involves a virtually identical power spectral density, and a comparison of (4.21) and (4.25) shows that

$$\Phi_{\mathrm{q}} \sim \frac{V_{\mathrm{I}}}{\Delta^3} \Phi_{\mathrm{d}}. \quad (4.26)$$

The introduction of a LEBU leads to a reduction in the quadrupole pressure spectrum in (4.24) since it reduces the amplitude of the velocity fluctuations and decreases the integral lengthscale of the turbulence (Coustols *et al.* 1987). However, when the LEBU is present we also have a dipole sound field with a pressure spectrum

described by (4.19). Equation (4.26) and a comparison of (4.19) and (4.24) show that this dipole field is negligible in comparison with the quadrupole field provided that

$$\frac{l_{\mathrm{I}} l^3}{\pi |\boldsymbol{x}|^2} \min(L, |\boldsymbol{x}|) \ll \left(\frac{\omega \Delta}{c}\right)^2 V_{\mathrm{I}} \ln\left(\frac{8\omega D}{\pi c}\right), \tag{4.27}$$

A typical LEBU has a chord of the order of the boundary-layer thickness, $2l \sim \Delta$. The turbulence integral length l_{I} also scales on the boundary-layer thickness and the integral correlation volume V_{I} scales on Δ^3. Hence (4.27) simplifies to

$$\frac{\min(L, |\boldsymbol{x}|)}{8\pi\Delta} \ll \left(\frac{\omega |\boldsymbol{x}|}{c}\right)^2 \ln\left(\frac{8\omega D}{\pi c}\right). \tag{4.28}$$

At positions $\boldsymbol{x}$ on the surface that are sufficiently far from the LEBU for the inequality in (4.28) to be satisfied the contribution to the surface pressure spectrum from the dipole source is negligible in comparison with that from the quadrupole. The logarithm in (4.28) only varies slowly with its argument and is typically of order unity.

Let us consider now an array of LEBUs mounted on a surface to produce global reductions in fluctuating velocity. This could be achieved by installing LEBUs which span the boundary-layer width and have an axial separation of, say, 150Δ. Such an arrangement would modify the turbulence and reduce the quadrupole components of the surface pressure spectrum. Provided that the dipole sound is less than this quadrupole field, this would lead to a reduction in the flow noise. It is apparent from (4.28) that such a reduction can only be obtained in a region midway between the LEBUs provided that

$$\frac{1}{4\pi} \ll 75 \left(\frac{\omega \Delta}{c}\right)^2. \tag{4.29}$$

Hence, at frequencies less than $c/30\Delta$ the installation of LEBUs will increase the flow noise because they introduce new dipole sources which produce more intense sound than the quadrupole sources in an unmanipulated layer. The introduction of LEBUs could only have a beneficial effect and lead to local reductions in the surface pressure spectrum at radian frequencies which are large in comparison with $c/30\Delta$. Even then, if V_{I} is significantly less than Δ^3 for these high-frequency disturbances, (4.28) underestimates the relative magnitude of the dipole sound due to the LEBUs and they may still have an adverse effect.

5. Conclusions

The idealized problem of a two-dimensional elliptical vortex convected past a LEBU has been solved exactly in the low-Mach-number limit. The inner incompressible unsteady pressure is increased by the large factor $U_\infty h/\Gamma$ by the introduction of a LEBU. The augmented wall pressure is most intense directly underneath the LEBU, the maximum being below the 20% chord point. In an unmanipulated flow the far-field pressure is proportional to the small eccentricity, ϵ, of the vortex core. All vortical elements satisfying Taylor's hypothesis are silent. When the vortex is convected past a LEBU even the frozen convected vorticity generates sound as it exerts an unsteady suction on the plate. The LEBU increases the distant acoustic pressure field by a factor $\epsilon^{-1}M^{-1}$. Since both ϵ and M are small this represents a considerable augmentation in the sound of a single eddy.

When a LEBU is placed in a turbulent boundary layer, the suction force on the

LEBU generates dipole sound in addition to that produced by the Lighthill quadrupole sources distributed throughout the boundary layer. The dipole field decays with distance from the LEBU and we find that, at positions sufficiently far from the LEBU that the inequality in (4.27) is satisfied, the pressures induced by the dipole field are negligible in comparison with those due to the volume quadrupoles.

An array of LEBUs, mounted over a surface to produce global reductions in turbulent velocity, can only lead to local reductions in flow noise for radian frequencies much greater than $c/30\Delta$.

This work has been carried out with the support of Topexpress Ltd and the Procurement Executive, Ministry of Defence.

Appendix A. Evaluation of inner incompressible surface pressure perturbation near a LEBU

After differentiation with respect to time and linearization in the vortex strength Γ, equation (2.16) leads to

$$\dot{\phi}(y_1,0,y_3,t) = -\frac{1}{\pi}\frac{\Gamma U_\infty d}{(y_1-U_\infty t)^2+d^2}+\frac{1}{\pi}\int_{-l}^{l}\dot{f}(y_1',t)\,\Theta(y_1,0\,|\,y_1',h)\,\mathrm{d}y_1' + \frac{1}{\pi}\int_0^\infty \dot{\gamma}_w(s,t)\,\Theta(y_1,0\,|\,s+l,h)\,\mathrm{d}s. \quad \text{(A 1)}$$

This expression for the rate of change of velocity potential can be simplified.

First note that differentiation of the circulation theorem in (2.12) with respect to time shows that

$$\int_0^\infty \dot{\gamma}_w(s,t)\,\mathrm{d}s = -\int_{-l}^{l}\dot{f}(y_1',t)\,\mathrm{d}y_1'. \quad \text{(A 2)}$$

Once (2.17) has been used to express $\dot{\gamma}_w$ in terms of $\partial\gamma_w/\partial s$, the s-integral may be evaluated to give

$$\gamma_w(0,t) = -\frac{1}{U_\infty}\int_{-l}^{l}\dot{f}(y_1',t)\,\mathrm{d}y_1'. \quad \text{(A 3)}$$

The last integral in the expression for the velocity potential, (A 1), may be simplified in a similar way. With $\dot{\gamma}_w$ replaced by $-U_\infty\,\partial\gamma_w/\partial s$, a straightforward integration by parts leads to

$$\int_0^\infty \dot{\gamma}_w(s,t)\,\Theta(y_1,0\,|\,s+l,h)\,\mathrm{d}s = -U_\infty\int_0^\infty \frac{\gamma_w(s,t)\,h\,\mathrm{d}s}{(y_1-s-l)^2+h^2}+U_\infty\,\gamma_w(0,t)\,\Theta(y_1,0\,|\,l,h), \quad \text{(A 4)}$$

since $\partial\Theta/\partial s = -h/((y_1-s-l)^2+h^2)$.

It would be convenient to rearrange the second integral in (A 1) in a similar way. This can be done by introducing a new function $g(y_1,t)$ defined by

$$g(y_1,t) = \int_{-l}^{y_1}\dot{f}(y_1',t)\,\mathrm{d}y_1'. \quad \text{(A 5)}$$

The definition ensures that $g(-l,t)$ vanishes, and an integration by parts gives

$$\int_{-l}^{l}\dot{f}(y_1',t)\,\Theta(y_1,0\,|\,y_1',h)\,\mathrm{d}y_1' = \int_{-l}^{l}\frac{g(y_1',t)\,h\,\mathrm{d}y_1'}{(y_1-y_1')^2+h^2}+g(l,t)\,\Theta(y_1,0\,|\,l,h). \quad \text{(A 6)}$$

Substitution from (A 4) and (A 6) into (A 1) leads to

$$\dot{\phi} = -\frac{1}{\pi}\frac{\Gamma U_\infty d}{(y_1 - U_\infty t)^2 + d^2} + \frac{1}{\pi}\int_{-l}^{l} \frac{g(y_1', t)\, h\, \mathrm{d}y_1'}{(y_1 - y_1')^2 + h^2} - \frac{U_\infty}{\pi}\int_0^\infty \frac{\gamma(s,t)\, h\, \mathrm{d}s}{(y_1 - s - l)^2 + h^2} + \frac{1}{\pi}\Theta(y_1, 0 \mid l, h)\,[g(l,t) + U_\infty \gamma_w(0,t)]. \quad \text{(A 7)}$$

It follows from the definition of g that

$$g(l,t) = \int_{-l}^{l} \dot{f}(y_1', t)\, \mathrm{d}y_1'.$$

The circulation theorem expressed in (A 3) therefore shows that the last term in (A 7) vanishes and $\dot{\phi}$ has quite a simple form.

On $y_2 = 0$, v_2 is identically zero and, after linearization, v_1 in (2.15) simplifies to

$$v_1 = U_\infty + \frac{1}{\pi}\frac{\Gamma d}{(y_1 - U_\infty t)^2 + d^2} + \frac{1}{\pi}\int_{-l}^{l} \frac{f(y', t)\, h\, \mathrm{d}y_1'}{(y_1 - y_1')^2 + h^2} + \frac{1}{\pi}\int_0^\infty \frac{\gamma_w(s,t)\, h\, \mathrm{d}s}{(y_1 - s - l)^2 + h^2}. \quad \text{(A 8)}$$

Substitution for $\dot{\phi}$ and v_1 from (A 7) and (A 8) into the unsteady Bernoulli equation (2.6) leads to an expression for the surface pressure fluctuation:

$$p'(y_1, 0, y_3, t) = -\frac{\rho_0 h}{\pi}\int_{-l}^{l} \frac{g(y_1', t) + U_\infty f(y_1', t)}{(y_1 - y_1')^2 + h^2}\, \mathrm{d}y_1', \quad \text{(A 9)}$$

which is used in (2.18).

Appendix B. Evaluation of the integrals in the representation for the distant pressure field

We shall begin by evaluating the surface integrals in the representations (3.17) and (3.18) for the far-field pressure. These are of form $\int [n_i r^{-2} \phi]\, \mathrm{d}S$ and $\int [n_i y_j r^{-3} \phi]\, \mathrm{d}S$, where $r = |\boldsymbol{x} - y_3 \boldsymbol{k}|$ and the square brackets denote that the function they enclose is to be evaluated at retarded time $t - r/c$. We shall evaluate these integrals in a similar way to the standard proof of the Blasius theorems (see for example Duncan, Thom & Young 1970).

Consider first the complex integral

$$\int (n_2 \phi - \mathrm{i} n_1 \phi)\, \mathrm{d}s, \quad \text{(B 1)}$$

where $\boldsymbol{n}$ denotes the inward normal and s is arclength around the two-dimensional body. We introduce the complex position variable $z = y_1 + \mathrm{i} y_2$. Then, for an incremental $\mathrm{d}z$ tangential to the body,

$$\mathrm{d}z = (n_2 - \mathrm{i} n_1)\, \mathrm{d}s, \quad \text{(B 2)}$$

and hence the integral in (B 1) can be written as

$$\int (n_2 \phi - \mathrm{i} n_1 \phi)\, \mathrm{d}s = \oint \phi\, \mathrm{d}z. \quad \text{(B 3)}$$

Since the body surface is a streamline, the stream function ψ has a constant value, ψ_c say, on the body and

$$\oint \psi\, \mathrm{d}z = \psi_c \oint \mathrm{d}z = 0. \quad \text{(B 4)}$$

After combining (B 3) and (B 4) we obtain

$$\int (n_2\phi - \mathrm{i}n_1\phi)\,\mathrm{d}s = \oint w\,\mathrm{d}z, \tag{B 5}$$

where $w(z)$ is the complex potential $\phi + \mathrm{i}\psi$. Equation (2.16) shows that near the plate and outside the vortex core this complex potential is given by

$$\begin{aligned} w(z) = U_\infty z - \frac{\mathrm{i}\Gamma}{2\pi}(\ln(z - y_{v1} - \mathrm{i}y_{v2}) - \ln(z - y_{v1} + \mathrm{i}y_{v2})) \\ - \frac{\mathrm{i}}{2\pi}\int_{-l}^{l} f(y_1', t)\,(\ln(z - y_1' - \mathrm{i}h) - ln(z - y_1' + \mathrm{i}h))\,\mathrm{d}y_1' \\ - \frac{\mathrm{i}}{2\pi}\int_0^\infty \gamma_w(s,t)\,(\ln(z - y_{w1} - \mathrm{i}y_{w2}) - \ln(z - y_{w1} + \mathrm{i}y_{w2}))\,\mathrm{d}s. \end{aligned} \tag{B 6}$$

After substitution for $w(z)$ from (B 6) into (B 5) we find that the z-integral involves terms of the form $\oint \ln(z - z')\,\mathrm{d}z$. If z' is outside the body this integral is identically zero, while for a position z' within the body, the integral reduces to a branch-cut integral which can be readily evaluated. This leads to

$$\int (n_2\phi - \mathrm{i}n_1\phi)\,\mathrm{d}s = \int_{-l}^{l} (l - y_1')f(y_1', t)\,\mathrm{d}y_1'. \tag{B 7}$$

The imaginary part of (B 7) shows that

$$\int n_1\phi\,\mathrm{d}s = 0, \tag{B 8}$$

and, after integration over y_3, it follows that

$$\int_S \frac{[n_1\phi]}{r^2}\,\mathrm{d}S = 0; \tag{B 9}$$

a result that we shall use later.

The LEBU is positioned at $y_2 = h$ and so

$$\frac{\partial}{\partial t}\int_S \frac{[y_2 n_2\phi]}{r^3}\,\mathrm{d}S = h\int_{-\infty}^{\infty} \frac{\mathrm{d}y_3}{r^3}\int_{-l}^{l} [n_2\dot{\phi}]\,\mathrm{d}s. \tag{B 10}$$

The s-integral has been evaluated as the real part of (B 7) and shows that

$$\frac{\partial}{\partial t}\int_S \frac{[y_2 n_2\phi]}{r^3}\,\mathrm{d}S = h\int_{-\infty}^{\infty} \frac{\mathrm{d}y_3}{r^3}\int_{-l}^{l} (l - y_1')\dot{f}(y_1', t - r/c)\,\mathrm{d}y_1'. \tag{B 11}$$

After integration by parts this becomes

$$\frac{\partial}{\partial t}\int_S \frac{[y_2 n_2\phi]}{r^3}\,\mathrm{d}S = h\int_{-\infty}^{\infty} \frac{\mathrm{d}y_3}{r^3}\int_{-l}^{l} g(y_1', t - r/c)\,\mathrm{d}y_1', \tag{B 12}$$

where the function g has been defined in (2.19).

The final surface integral in the representation (3.18) for the far-field quadrupole pressure is

$$\int_S \frac{[y_1 n_1\phi]}{r^3}\,\mathrm{d}S. \tag{B 13}$$

This may be evaluated in a similar way by considering the complex integral

$$\int z(n_2\phi - \mathrm{i}n_1\phi)\,\mathrm{d}s. \tag{B 14}$$

Such a procedure shows that the integral in (B 13) vanishes.

We showed in (B 9) that

$$\int_S \frac{[n_1 \phi]}{r^2} \mathrm{d}S = 0.$$

The dipole strength in (3.17) therefore only depends on the volume integral $\int ([v_2 \omega_3]/r^2)\, \mathrm{d}^3 y$. Vorticity is concentrated within the vortex core and the plate wake, and substitution for ω_3 from (2.13) and for the variation of v_2 over the vortex core from (2.14) shows that

$$\int v_2 \omega_3 \, \mathrm{d}y_1 \, \mathrm{d}y_2 = \tfrac{1}{2}\omega^2 \int H(a + \epsilon a \cos(2\Theta_1 - \tfrac{1}{2}\omega t) - R_1)\, R_1(\cos\Theta_1 - \epsilon \cos(\theta_1 - \tfrac{1}{2}\omega t))\, \mathrm{d}y_1 \, \mathrm{d}y_2 + \Gamma v_2(\boldsymbol{y}_\mathrm{v}(t), t) + \int_{s=0}^{\infty} \gamma_\mathrm{w}(s,t)\, v_2(\boldsymbol{y}_\mathrm{w}(s,t), t)\, \mathrm{d}s. \quad \text{(B 15)}$$

The first integral can be evaluated in a straightforward way and is found to be identically zero. When v_2 is substituted from (2.14) and (2.15) into (B 15), two terms cancel to give

$$\begin{aligned}\int v_2 \omega_3 \, \mathrm{d}y_1 \, \mathrm{d}y_2 = {} & \frac{\Gamma}{2\pi} \int_{-l}^{l} f(y_1, t) \{E_2(\boldsymbol{y}_\mathrm{v} \mid y_1, h) - E_2(\boldsymbol{y}_\mathrm{v} \mid y_1, -h)\}\, \mathrm{d}y_1 \\ & + \frac{1}{2\pi} \int_{-l}^{l} f(y_1, t) \int_0^\infty \gamma_\mathrm{w}(s,t) \{E_2(\boldsymbol{y}_\mathrm{w} \mid y_1, h) - E_2(\boldsymbol{y}_\mathrm{w} \mid y_1, -h)\}\, \mathrm{d}s \, \mathrm{d}y_1 \\ & + \frac{1}{2\pi} \int_0^\infty \gamma_\mathrm{w}(s,t) \int_0^\infty \gamma_\mathrm{w}(s',t) \{E_2(\boldsymbol{y}_\mathrm{w} \mid \boldsymbol{y}'_\mathrm{w}) - E_2(\boldsymbol{y}_\mathrm{w} \mid y'_{\mathrm{w}1}, -y'_{\mathrm{w}2})\}\, \mathrm{d}s' \, \mathrm{d}s. \end{aligned} \quad \text{(B 16)}$$

The function $E_2(\boldsymbol{y} \mid \boldsymbol{y}')$ is defined by $E_2(\boldsymbol{y} \mid \boldsymbol{y}') = (y_1 - y'_1)/((y_1 - y'_1)^2 + (y_2 - y'_2)^2)$. The symmetry in this expression shows that

$$E_2(\boldsymbol{y} \mid \boldsymbol{y}') = -E_2(\boldsymbol{y}' \mid \boldsymbol{y}), \quad E_2(y_1, -y_2 \mid y'_1, -y'_2) = E_2(\boldsymbol{y} \mid \boldsymbol{y}'). \quad \text{(B 17)}$$

Now, since the plate is impenetrable, the normal fluid velocity on it vanishes, i.e.

$$v_2(\boldsymbol{y}, t) = 0 \quad \text{for} \quad -l \leqslant y_1 \leqslant l, \quad y_2 = h. \quad \text{(B 18)}$$

The form for v_2 in (2.15) and the relationships in (B 17) show that this condition is equivalent to

$$\begin{aligned} & \Gamma\{E_2(\boldsymbol{y}_\mathrm{v} \mid y_1, h) - E_2(\boldsymbol{y}_\mathrm{v} \mid y_1, -h)\} + \int_0^\infty \gamma_\mathrm{w}(s,t) \{E_2(\boldsymbol{y}_\mathrm{w} \mid y_1, h) - E_2(\boldsymbol{y}_\mathrm{w} \mid y_1, -h)\}\, \mathrm{d}s \\ & \quad = \int_{-l}^{l} f(y'_1, t) \left\{ \frac{1}{y_1 - y'_1} - \frac{y_1 - y'_1}{(y_1 - y'_1)^2 + 4h^2} \right\} \mathrm{d}y'_1 \quad \text{for} \quad -l \leqslant y_1 \leqslant l. \end{aligned} \quad \text{(B 19)}$$

This identity may be used to simplify the first two integrals in (B 16):

$$\begin{aligned} \int v_2 \omega_3 \, \mathrm{d}y_1 \, \mathrm{d}y_2 = {} & \frac{1}{2\pi} \int_{-l}^{l} f(y_1, t) \int_{-l}^{l} f(y'_1, t) \left\{ \frac{1}{y_1 - y'_1} - \frac{y_1 - y'_1}{(y_1 - y'_1)^2 + 4h^2} \right\} \mathrm{d}y'_1 \, \mathrm{d}y_1 \\ & + \frac{1}{2\pi} \int_0^\infty \gamma_\mathrm{w}(s,t) \int_0^\infty \gamma_\mathrm{w}(s',t) \{E_2(\boldsymbol{y}_\mathrm{w} \mid \boldsymbol{y}'_\mathrm{w}) - E_2(\boldsymbol{y}_\mathrm{w} \mid y'_{\mathrm{w}1}, -y'_{\mathrm{w}2})\}\, \mathrm{d}s' \, \mathrm{d}s. \end{aligned} \quad \text{(B 20)}$$

$\gamma_\mathrm{w}(s', t)$ is a non-singular function and the order of integration in the last term in (B 20) can be exchanged. Such a procedure shows that

$$\begin{aligned} I &= \int_0^\infty \gamma_\mathrm{w}(s,t) \int_0^\infty \gamma_\mathrm{w}(s',t) \{E_2(\boldsymbol{y}_\mathrm{w} \mid \boldsymbol{y}'_\mathrm{w}) - E_2(\boldsymbol{y}_\mathrm{w} \mid y'_{\mathrm{w}1}, -y'_{\mathrm{w}2})\}\, \mathrm{d}s' \, \mathrm{d}s \\ &= \int_0^\infty \gamma_\mathrm{w}(s',t) \int_0^\infty \gamma_\mathrm{w}(s,t) \{E_2(\boldsymbol{y}_\mathrm{w} \mid \boldsymbol{y}'_\mathrm{w}) - E_2(\boldsymbol{y}_\mathrm{w} \mid y'_{\mathrm{w}1}, -y'_{\mathrm{w}2})\}\, \mathrm{d}s \, \mathrm{d}s'. \end{aligned} \quad \text{(B 21)}$$

The relationships in (B 17) show that

$$E_2(y_w|y'_w) = -E_2(y'_w|y) \quad \text{and} \quad E_2(y_w|y'_{w1}, -y'_{w2}) = -E_2(y'_w|y_{w1}, -y_{w2}).$$

Hence

$$I = -\int_0^\infty \gamma_w(s',t) \int_0^\infty \gamma_w(s,t)\{E_2(y'_w|y_w) - E_2(y'_w|y_{w1}, -y_{w2})\}\,ds\,ds'. \tag{B 22}$$

After exchanging the names of the integration variables s and s', the integral on the right-hand side of (B 22) is precisely the same as that defining I in (B 21). Hence combining (B 21) and (B 22) leads to

$$I = -I, \tag{B 23}$$

and we must conclude that

$$I = 0. \tag{B 24}$$

The last integral in (B 20) vanishes.

A similar argument shows that

$$\int_{-l}^{l} f(y_1,t) \int_{-l}^{l} \frac{f(y'_1,t)\,(y_1-y'_1)}{(y_1-y'_1)^2+4h^2}\,dy'_1\,dy_1 = 0, \tag{B 25}$$

and (3.20) simplifies to

$$\int v_2\omega_3\,dy_1\,dy_2 = \frac{1}{2\pi}\int_{-l}^{l} f(y_1,t) \oint_{-l}^{l} \frac{f(y'_1,t)}{y_1-y'_1}\,dy'_1\,dy_1. \tag{B 26}$$

The same argument cannot be applied to the integrals remaining in (B 26) because f has a singularity at the leading edge and the y'_1 integral exists only as a principal value. These integrals need to be evaluated explicitly. However, we note that, since the leading-edge singularity prevents the integral in (B 26) from being zero, we expect the integral to be proportional to $A_0^2(t)$, because $A_0(t)$ is the coefficient of the singular term in the Glauert series.

Substitution for f in terms of its Glauert series (2.11) enables the remaining integrals in (B 26) to be evaluated explicitly. It shows that

$$\oint_{-l}^{l} \frac{f(y'_1,t)}{y_1-y'_1}\,dy'_1 = \left[(l+y_1)\log\left(\frac{l+y_1}{l-y_1}\right) - 2l\right]\frac{f(l,t)}{2l} - \frac{\pi\Gamma}{l}\left(\tfrac{1}{2}A_0(t) + \sum_{n=1}^{\infty} A_n(t)\cos n\theta\right), \tag{B 27}$$

where $\cos\theta = -y_1/l$ and the Glauert integral

$$\oint_0^\pi \frac{\cos n\theta'}{\cos\theta'-\cos\theta}\,d\theta' = \frac{\pi\sin n\theta}{\sin\theta}$$

has been used. Finally, after multiplying the right-hand side of (B 27) by the Glauert series for $f(y_1,t)$ and integrating with respect to y_1, we find

$$\int v_2\omega_3\,dy_1\,dy_2 = \frac{\pi\Gamma^2}{8l}A_0^2(t). \tag{B 28}$$

As expected, the strength of the dipole is proportional to $A_0^2(t)$ and leads to a sound field

$$p'_d(\boldsymbol{x},t) = \frac{\rho_0 x_1 \Gamma^2}{16cl}\frac{\partial}{\partial t}\int \frac{A_0^2(t-r/c)}{r^2}\,dy_3. \tag{B 29}$$

This result is used in (3.19).

We now turn our attention to the quadrupole sound in (3.18). Since we already have a second-order dipole we shall only evaluate the quadrupole source strength to first order in Γ. The integrals over the surface of the LEBU have already been evaluated. In particular, from (B 12) and (B 13) we have

$$\frac{\partial}{\partial t}\int_S \left[\frac{y_2 n_2 \phi}{r^3}\right] \mathrm{d}S = h\int_{-\infty}^{\infty} \frac{\mathrm{d}y_3}{r^2}\int_{-l}^{l} g(y_2, t-r/c)\,\mathrm{d}y_1, \tag{B 30}$$

and

$$\int_S \left[\frac{y_1 n_1 \phi}{r^3}\right] \mathrm{d}S = 0. \tag{B 31}$$

The volume integrals describing the quadrupole source strength simplify considerably when they are linearized. To lowest order in Γ, we find that

$$\int y_1 v_2 \omega_3 \,\mathrm{d}y_1\,\mathrm{d}y_2 = 0, \tag{B 32}$$

while

$$\int y_2 v_1 \omega_3 \,\mathrm{d}y_1\,\mathrm{d}y_2 = U_\infty(h+b)\,\Gamma + U_\infty h\int_0^\infty \gamma_w(s,t)\,\mathrm{d}s. \tag{B 33}$$

The circulation theorem expressed in (2.12) enables the total vorticity in the wake to be expressed in terms of the circulation around the plate, so that

$$\int y_2 v_1 \omega_3 \,\mathrm{d}y_1\,\mathrm{d}y_2 = U_\infty(h+b)\,\Gamma - U_\infty h\int_{-l}^{l} f(y_1,t)\,\mathrm{d}y_1. \tag{B 34}$$

Substitution of (B 30) and (B 34) into (3.18) shows that the quadrupole is in the 2–2 direction, and leads to a pressure field

$$p'_{\mathrm{q}}(\boldsymbol{x},t) = \frac{\rho_0 x_2^2 h}{2\pi c^2}\frac{\partial^2}{\partial t^2}\int_{-\infty}^{\infty}\frac{\mathrm{d}y_3}{r^3}\int_{-l}^{l}\left(g(y_1,t-r/c)+U_\infty f(y_1,t-r/c)\right)\mathrm{d}y_1, \tag{B 35}$$

a result that is used in (3.20).

Appendix C. Evaluation of the unsteady force on the LEBU

The forces exerted on an isolated plate in a gust have been considered extensively (see for example Glauert 1929; Sears 1940; Jones 1957). In our geometry the plate or LEBU is positioned above an infinite plane wall, but nevertheless we can obtain simple expressions for the force. Let (X, Y) denote the force exerted on the fluid by unit spanwise length of LEBU. Then

$$Y + \mathrm{i}X = -\int (n_2 + \mathrm{i}n_1)\, p\,\mathrm{d}s. \tag{C 1}$$

The unsteady form of Bernoulli's equation shows that in this inner incompressible flow

$$p = -\rho_0\frac{\partial\phi}{\partial t} - \tfrac{1}{2}\rho_0 v^2 + \text{constant}. \tag{C 2}$$

When this is used to substitute for the pressure, the integral in (C 1) can be written in complex form as

$$Y + \mathrm{i}X = \overline{\rho_0 \oint \frac{\partial w}{\partial t}\,\mathrm{d}z} + \tfrac{1}{2}\rho_0 \oint \left(\frac{\partial w}{\partial z}\right)^2 \mathrm{d}z, \tag{C 3}$$

where the overbar denotes a complex conjugate. We have already considered the first integral in this equation (see (B 5) and (B 7)). When w in (B 6) has been differentiated

with respect to z, the second integral has a straightforward form and can be readily evaluated to show that

$$X = \frac{\rho_0}{2\pi}\int_{-l}^{l} f(y_1,t)\left\{\Gamma E_2(y_v\,|\,y_1,h) - \Gamma E_2(y_v\,|\,y_1,-h) - \int_{-l}^{l}\frac{f(y_1',t)\,(y_1'-y_1)}{(y_1'-y_1)^2+4h^2}\,\mathrm{d}y_1' + \int_0^\infty \gamma_w(s,t)\,(E_2(y_w\,|\,y_1,h) - E_2(y_w\,|\,y_1,-h))\,\mathrm{d}s\right\}\mathrm{d}y_1. \quad \text{(C 4)}$$

The condition that the plate is impenetrable, expressed mathematically in (B 19), enables this integral to be simplified to

$$X = \frac{\rho_0}{2\pi}\int_{-l}^{l} f(y_1,t)\int_{-l}^{l}\frac{f(y_1',t)}{y_1-y_1'}\,\mathrm{d}y_1'\,\mathrm{d}y_1. \quad \text{(C 5)}$$

This integral was evaluated in Appendix B where the steps between (B 26) and (B 28) show it to be equal to $\rho_0\pi\Gamma^2A_0^2(t)/8l$. The plate exerts a thrust on the fluid, proportional to the square of the oncoming velocity fluctuations.

After linearization in Γ, the strength of the oncoming vortex, the real part of (C 3) shows that

$$Y = \rho_0\int_{-l}^{l}(g(y_1,t) + U_\infty f(y_1,t))\,\mathrm{d}y_1. \quad \text{(C 6)}$$

The leading term in the unsteady lift force depends linearly on the velocity fluctuations.

REFERENCES

Atassi, H. M. & Gebert, G. A. 1987 Modification of turbulent boundary layer structure by large-eddy breakup devices. In *Proc. Turbulent Drag Reduction by Passive Means*, vol. 2, pp. 432–456. R. Aero. Soc.

Balakumar, P. & Widnall, S. E. 1986 Application of unsteady aerodynamics to large-eddy breakup devices in a turbulent flow. *Phys. Fluids* **29**, 1779–1787.

Bandyopadhyay, P. R. 1986 Review – Mean flow in turbulent boundary layers disturbed to alter skin friction. *Trans. ASME* I: *J. Fluids Engng* **108**, 127–140.

Beeler, G. B. 1986 Turbulent boundary layer wall pressure fluctuations downstream of a tandem LEBU. *AIAA J.* **24**, 689–691.

Bergeron, R. F. 1973 Aerodynamic sound and the low wavenumber wall pressure spectrum of nearly incompressible boundary layer turbulence. *J. Acoust. Soc. Am.* **55**, 123–133.

Bertelrud, A. 1986 Manipulated turbulence structure in flight. In *Advances in Turbulence*, pp. 524–532. Springer.

Bonnet, J. P., Delville, J. & Lemay, J. 1987 Study of LEBUs modified turbulent boundary layer by use of passive temperature contamination. In *Proc. Turbulent Drag Reduction by Passive Means*, vol. 1, pp. 45–68. R. Aero. Soc.

Corke, T. C., Guezennec, Y. G. & Nagib, H. M. 1979 Modification in drag of turbulent boundary layers resulting from manipulation of large-scale structures. In *Proc. Viscous Drag Reduction Symp., Dallas. AIAA Prog. Astro. Aero.* **72**, 128–143.

Coustols, E., Cousteix, J. & Belanger, J. 1987 Drag reduction performance on riblet surfaces and through outer layer manipulators. In *Proc. Turbulent Drag Reduction by Passive Means*, vol. 2, pp. 250–289. R. Aero. Soc.

Dowling, A. P. 1985 The effect of large-eddy breakup devices on oncoming vorticity. *J. Fluid Mech.* **160**, 447–463.

Duncan, W. J., Thom, A. S. & Young, A. D. 1970 *Mechanics of Fluids*, 2nd edn. Arnold.

Ffowcs Williams, J. E. 1965 Surface-pressure fluctuations in the turbulent flow over a flat plate. *J. Fluid Mech.* **22**, 507–519.

Ffowcs Williams, J. E. 1969 Hydrodynamic noise. *Ann. Rev. Fluid Mech.* **1**, 197–222.

FFOWCS WILLIAMS, J. E. 1982 Boundary-layer pressures and the Corcos model: a development to incorporate low-wavenumber constraints. *J. Fluid Mech.* **125**, 9–25.

FFOWCS WILLIAMS, J. E. & HAWKINGS, D. L. 1969 Sound generation by turbulence and surfaces in arbitrary motion. *Phil. Trans. R. Soc. Lond.* A**264**, 321–342.

GLAUERT, H. 1929 The force and moment on an oscillating aerofoil. *Aero. Res. Counc. R. & M.* 1242.

GRADSHTEYN, I. S. & RYZHIK, I. M. 1980 *Tables of Integrals, Series and Products.* Academic.

GUEZENNEC, Y. G. & NAGIB, H. M. 1985 Documentation of mechanisms leading to net drag reduction in manipulated turbulent boundary layers. *AIAA*-85-0519.

HEFNER, J. N., WEINSTEIN, L. M. & BUSHNELL, D. M. 1979 Large-eddy breakup scheme for turbulent viscous drag reduction. In *Proc. Viscous Drag Reduction Symp., Dallas. AIAA Prog. Astro. Aero.* **72**, 110–127.

HOWE, M. S. 1975 Contributions to the theory of aerodynamic sound, with application to excess jet noise and the theory of the flute. *J. Fluid Mech.* **71**, 625–673.

HOWE, M. S. 1976 The influence of vortex shedding on the generation of sound by convected turbulence. *J. Fluid Mech.* **76**, 711–740.

HOWE, M. S. 1987 On the structure of the turbulent boundary layer wall pressure spectrum in the vicinity of the acoustic wavenumber. *Proc. R. Soc. Lond.* A**412**, 389–401.

JONES, D. S. 1957 The unsteady motion of a thin aerofoil in an incompressible fluid. *Commun. Pure Appl. Maths* **10**, 1–21.

KATZMAYER, R. 1922 Effect of periodic changes of angle of attack on behaviour of airfoils. *NACA PM*147.

LAMB, H. 1932 *Hydrodynamics.* Cambridge University Press.

NGUYEN, V. D., DICKINSON, J., JEAN, Y., CHALIFOUR, Y., ANDERSON, J., LEMAY, J., HAEBERLE, D. & LAROSE, G. 1984 Some experimental observations of the law of the wall behind large-eddy breakup devices using servo-controller skin friction balances. *AIAA*-84-0346.

NGUYEN, V. D., SAVILL, A. M. & WESTPHAL, R. V. 1986 Skin friction measurements following manipulation of a turbulent boundary layer. *AIAA J.* **25**, 498–500.

PLESNIAK, M. W. & NAGIB, H. M. 1985 Net drag reduction in turbulent boundary layers resulting from optimized manipulation. *AIAA*-85-0518.

POWELL, A. 1964 Theory of vortex sound. *J. Acoust. Soc. Am.* **36**, 177–195.

SAHLIN, A., ALFREDSSON, P. H. & JOHANSSON, A. V. 1986 Direct drag measurements for a flat plate with passive boundary layer manipulators. *Phys. Fluids* **29**, 696–700.

SEARS, W. R. 1940 Some aspects of non-stationary airfoil theory and its practical application. *J. Aero. Sci.* **8**, 104–108.

SEVIK, M. M. 1986 Topics in hydro-acoustics. *IUTAM Symp. on Aero- and Hydro-Acoustics, Lyon/France.* Springer.

WESTPHAL, R. V. 1986 Skin friction and Reynolds Stress measurements for a turbulent boundary layer following manipulation using flat plates. *AIAA*-86-0283.

WILKINSON, S. P., ANDERS, J. B., LAZOS, B. S. & BUSHNELL, D. M. 1987 Turbulent drag reduction research at NASA Langley – Progress and Plans. In *Proc. Turbulent Drag Reduction by Passive Means*, vol. 1, pp. 1–32. R. Aero. Soc.